

1 **TRANSCRIPTOMIC SIGNATURES OF TELOMERASE-DEPENDENT AND -INDEPENDENT**
2 **AGEING, IN THE ZEBRAFISH GUT AND BRAIN**

3 *Running title: Kinetics of ageing in the zebrafish gut and brain*

4
5 **AUTHORS**

6 Raquel R. Martins¹, Michael Rera² and Catarina M. Henriques¹

7 Affiliations :

8 1. The Bateson Centre, Healthy Lifespan Institute and Department of Oncology
9 and Metabolism, University of Sheffield Medical School, Sheffield, UK.

10 2. Université de Paris / Inserm- Centre de Recherche Interdisciplinaire (CRI Paris)

11

12 Corresponding author: c.m.henriques@sheffield.ac.uk

13

14 **SUMMARY**

15 Telomerase is best known for its role in the maintenance of telomere length and its
16 implications for ageing and cancer. The mechanisms, kinetics and tissue-specificity
17 underlying the protective or deleterious mechanisms of telomerase, however, remain
18 largely unknown. Here, we sought to determine the telomerase-dependent and -
19 independent transcriptomic changes with ageing, in the gut and brain, as examples of high
20 and low proliferative tissues, respectively. We hypothesised this could shed light on
21 common telomerase-dependent and -independent therapeutic targets aimed at preventing
22 or ameliorating age-associated dysfunction in both tissues. For this, we used the zebrafish
23 model which, similarly to humans, depends on telomerase for health- and lifespan. We
24 performed whole tissue RNA sequencing of gut and brain, in naturally aged zebrafish
25 alongside prematurely aged telomerase null mutants (*tert*^{-/-}), throughout their lifespan. Our
26 study highlights stem cell exhaustion as the first main hallmark of ageing to be de-regulated
27 in WT zebrafish gut and brain. Towards the end of life, altered intercellular communication
28 becomes the main hallmark of ageing de-regulated in both gut and brain, and this is
29 accelerated in both tissues, in the absence of telomerase. Finally, we identify 7 key gene
30 changes common between the gut and brain at the early stages of ageing, highlighting

31 potential early intervention therapeutic targets for preventing age-associated dysfunction in
32 both tissues.

33 **KEYWORDS:** Ageing, telomerase, telomeres, gut, brain, zebrafish, transcriptomics,
34 RNA sequencing

35 **1 INTRODUCTION**

36 Ageing is the strongest risk factor for chronic diseases. How and why this is the case
37 remain important questions in the field, especially as key research has shown that targeting
38 common hallmarks of ageing, such as cellular senescence (Baker et al., 2016; Baker et al.,
39 2011), can have a positive impact across multiple tissues and ameliorate several chronic
40 diseases of ageing at the same time. There are well-known key hallmarks of ageing, such as
41 genomic instability, telomere attrition, epigenetic alterations, loss of proteostasis, de-
42 regulated nutrient sensing, mitochondrial dysfunction, cellular senescence, stem cell
43 exhaustion and altered intercellular communication(Lemoine, 2021; López-Otín, Blasco,
44 Partridge, Serrano, & Kroemer, 2013) . However, a major challenge in ageing research is to
45 identify where and when these potentially pathological changes start and when the tipping
46 point between homeostasis and loss of function takes place (Rando & Wyss-Coray, 2021).
47 Additionally, several lines of evidence suggest there may be specific tissues where age-
48 related changes start earlier, potentially influencing others (de Jong, Gonzalez-Navajas, &
49 Jansen, 2016; Rera, Azizi, & Walker, 2013). One example is the gut, which has been
50 suggested to be a trigger for multiple organ failure (Cardoso et al., 2008). Evidence suggests
51 that the kinetics of ageing can vary dramatically between cells, tissues (Shokhirev &
52 Johnson, 2021; M. J. Zhang, Pisco, Darmanis, & Zou, 2021) and individuals, and that this is
53 influenced not only by intrinsic but also extrinsic factors, recently discussed elsewhere
54 (Rando & Wyss-Coray, 2021). These considerations are of particular importance when the
55 aim is to understand how changes in ageing lead to disease and how, when and where to
56 intervene. This is crucial in order to shift towards a more preventive form of medicine,
57 which is a current global ambition (Rudnicka et al., 2020), aiming to match the dramatic
58 increase of lifespan we have experienced in the past century, with an equivalent increase in
59 years of healthy living, i.e, healthspan (England, 2017).

60 Tissue-specific transcriptomics analysis over the lifecourse can offer important insights
61 into the downstream molecular mechanisms potentially driving the pathology of ageing.

62 Significant research is being dedicated to these approaches in different animal models,
63 including in mice (Schaum et al., 2020; Tabula Muris, 2020; M. J. Zhang et al., 2021).
64 Different animal models may offer different insights into the mechanisms of ageing, and
65 some models may be better suited to explore the role of specific human hallmarks of
66 ageing. The role of telomere attrition in natural ageing can be considered a hallmark of
67 ageing that may benefit from additional and complementary models, beyond the mouse
68 (Forsyth, Wright, & Shay, 2002; Gomes et al., 2011; Sullivan et al., 2021). Once such model is
69 the zebrafish that, like humans, age and die in a telomerase-dependent manner (Anchelin et
70 al., 2013; Carneiro, de Castro, & Ferreira, 2016; Madalena C Carneiro et al., 2016; Henriques,
71 Carneiro, Tenente, Jacinto, & Ferreira, 2013; Henriques & Ferreira, 2012). Restricted
72 telomerase expression and function are key determinants of natural ageing in humans,
73 underpinning multiple age-related diseases (Blackburn, Epel, & Lin, 2015). However, the role
74 and the dynamics of telomerase-dependent changes that may contribute to tissue-specific
75 ageing are still poorly understood. This is partially due to the fact that telomerase appears
76 to have multiple functions in the cell, that go beyond the maintenance of telomere length,
77 recently reviewed elsewhere (Segal-Bendirdjian & Geli, 2019).

78 Telomerase is best known for its telomere-dependent function (i.e. canonical
79 functions), acting as a reverse transcriptase, maintaining telomere length through its
80 catalytic domain (TERT protein) and RNA template (TERC) (Greider & Blackburn, 1985).
81 Telomeres are (TTAGGG)_n DNA repeats that together with a complex of proteins (known as
82 Shelterin) create a “cap-like” structure at the end of linear chromosomes (de Lange, 2004),
83 preventing the ends of linear chromosomes from being recognised as deleterious DNA
84 double strand breaks (Ferreira, Miller, & Cooper, 2004). However, in humans, due to time-
85 and cell-specific-limited telomerase expression, telomeres shorten with ageing, leading to
86 proliferative exhaustion and replicative senescence (Bodnar, 1998; d'Adda di Fagagna et al.,
87 2003). Importantly, there is accumulation of cellular senescence with ageing in humans
88 (Dimri et al., 1995) and senescence has been linked to several age-associated diseases
89 (Ovadya & Krizhanovsky, 2014). Additionally, short telomeres themselves can lead to de-
90 regulated gene expression, particularly in genes near the chromosome ends, due to loss of
91 the “telomere positioning effect” (TPE), which is known to regulate gene expression of
92 genes at least up to 10MB away from the chromosome ends (Robin et al., 2014).

93 Growing evidence now suggests that telomerase also has activity independent of its
94 action at telomeres, known as non-canonical (Goodman & Jain, 2011; Romaniuk et al., 2018;
95 Segal-Bendirdjian & Geli, 2019; Sung, Ali, & Lee, 2014). In the nucleus, these non-canonical
96 functions include transcriptional regulation of genes involved in inflammation, including
97 nuclear factor kappa B (NFkB) and tumour necrosis factor alpha (TNF α) (Deacon & Knox,
98 2018; Ghosh et al., 2012; Mattiussi, Tilman, Lenglez, & Decottignies, 2012), as well as genes
99 involved in cell proliferation (Choi et al., 2008; Sarin et al., 2005) and cell survival (Cao, Li,
100 Deb, & Liu, 2002; Rahman, Latonen, & Wiman, 2005). Telomerase can also translocate to
101 the mitochondria, where it has been shown to play a protective role against DNA damage
102 and oxidative stress (Ahmed et al., 2008; Haendeler et al., 2009).

103 As tissues with high cellular turnover present accelerated telomere erosion (Bodnar,
104 1998; H. W. Lee et al., 1998), it is reasonable to think that telomerase functions are likely to
105 primarily affect highly proliferative tissues. Accordingly, premature accumulation of critically
106 short telomeres has been identified in high proliferative tissues such as the gut, in tert-
107 deficient animal models. Nonetheless, the role of telomerase and telomeres is not restricted
108 to highly proliferative tissues. In the brain, considered a predominately post-mitotic tissue,
109 telomerase has been shown to have a protective role against excitotoxicity (Eitan et al.,
110 2012), oxidative stress (Spilsbury, Miwa, Attems, & Saretzki, 2015), and neuronal death (J.
111 Lee et al., 2010), all involved in neurodegenerative diseases. Studies in late-generation
112 telomerase-deficient mice have suggested that limited telomerase expression is associated
113 with premature accumulation of senescence-associated markers in different cell
114 populations including Purkinje neurons, cortical neurons and microglia (De Felice et al.,
115 2014; Jaskelioff et al., 2011; Jurk et al., 2012; Raj et al., 2015). Telomerase is therefore a
116 promising target to promote healthy ageing in multiple tissues and so the identification of
117 mechanisms driving telomerase-dependent ageing could enable the identification of
118 targeted therapies to improve healthspan.

119 In this study, we aimed to determine the telomerase-dependent and -independent
120 transcriptomic changes and their kinetics occurring during ageing, in both brain and gut
121 within the same individuals. We hypothesised that this would allow us to identify key age-
122 associated genes and pathways that become prematurely de-regulated in both or either
123 tissue, providing key insights into the early stages of ageing in these tissues and likely

124 interactions. We further hypothesised that this may highlight potential common
125 telomerase-dependent and -independent therapeutic targets for early intervention aimed at
126 preventing age-associated dysfunction in both tissues. To address these questions, we
127 performed RNA sequencing in whole tissues (gut and brain) of WT fish (2, 9, 22 and 35
128 months of age) alongside telomerase mutant fish (*tert*^{-/-}) (2, 9 and 22 months of age). *tert*^{-/-}
129 zebrafish, extensively characterised elsewhere (Anchelin et al., 2013; Madalena C Carneiro
130 et al., 2016; Henriques et al., 2013), display no telomerase activity and have significantly
131 shorter telomeres from birth, consequently ageing and dying prematurely. Ageing is usually
132 described as a time-dependent change in tissue homeostasis, that increases the probability
133 of disease and death (Hayflick, 2007). However, whether the genes and pathways driving or
134 accompanying these time-dependent changes are also consistently changing in a time-
135 specific manner, remains unresolved (Rando & Wyss-Coray, 2021). We therefore decided to
136 combine a time-series analysis (STEM), which allowed the identification of genes and
137 pathways that are consistently up or down-regulated over-time, with the more traditional
138 differential gene expression (DEGs) analysis between young and old animals. This combined
139 strategy allowed the identification of genes that change in a monotonic, time-dependent
140 manner (STEM), versus genes that change at specific stages of life (DEGs).

141 We show that although the gut and brain have distinct transcriptomic signatures of
142 ageing, both tissues display hallmarks of ageing as early as 9 months in the WT zebrafish.
143 Importantly, telomerase depletion accelerates the appearance of such hallmarks in both gut
144 and brain. In particular, we identify stem cell exhaustion as the common principal hallmark
145 of ageing at the early stages of ageing, in both tissues. Further, we identify altered
146 intercellular communication, in which immunity and inflammation play a central role, as the
147 main telomerase-dependent hallmark of ageing common between the gut and brain. Finally,
148 we conclude that the gut displays telomerase-dependent hallmarks of ageing at an earlier
149 age than the brain and that these include changes in several key genes that have also been
150 included in the GenAge database, a benchmark curated database that included genes
151 involved in ageing across different organisms, including in humans (Tacutu et al., 2018).
152 Finally, we identify 7 key gene changes common between the gut and brain at the early
153 stages of ageing, namely *ccnb1*, *kif2c*, *serpinh1a*, *temem37*, *si:ch211-5k11.8*, *cfap45* and
154 *eif4ebp3l*.

155

156 **2 RESULTS**

157 **2.1 Identification of monotonic, time-dependent gene signatures and process** 158 **changes with ageing in the zebrafish gut and brain**

159 In order to identify telomerase-dependent and -independent transcriptional
160 signatures of ageing in the zebrafish gut and brain, we performed RNA-Sequencing of whole
161 tissues, throughout the lifespan of WT and telomerase-deficient (*tert*^{-/-}) fish (**Fig. 1 and**
162 **source data**). While *tert*^{-/-} fish have a lifespan of c. 12-20 months, WT fish typically die
163 between c. 36-42 months of age (Madalena C Carneiro et al., 2016). The data shown here
164 include 4 age-groups of WT (2, 9, 22 and >30 months), corresponding to young, adult,
165 median lifespan and old. As the *tert*^{-/-} fish have a shorter lifespan compared with their WT
166 siblings, the data include 3 age-groups of telomerase-deficient fish (2, 9, and 22 months),
167 which correspond to young, medium lifespan and old. Each group has a sample size of 3
168 animals and the brains and guts from within the same groups of animals were used (**Fig 1A**).
169 The reads were aligned to the latest zebrafish genome build GRCz11 (Lawson et al., 2020)
170 and resulted in uniquely mapped read percentages ranging from 92.1% to 94.4%, which is a
171 readout of good quality (Lawson et al., 2020). All samples had at least 10 million uniquely
172 mapped reads, except G11 which had around 8 million. Further quality control, using a
173 principal component analysis (PCA) including all the samples, revealed that one of the gut
174 samples clustered with the brain samples, and not with the gut samples (**Fig. 1B**). This was
175 considered to be a technical error and this sample (G7) was therefore excluded from further
176 analysis. To analyse the overall impact of the genotype and age on transcriptomic
177 regulation, we then performed a PCA in the samples from the gut and brain, separately. We
178 further observed that some samples cluster *per* age, but there are some genotypes that
179 separate quite distinctly, despite being of the same age (**Fig 1C and D**). As an example, the
180 WT and *tert*^{-/-} gut samples are quite distinct, and the *tert*^{-/-} 2-month samples cluster closely
181 to the WT at 9 months than the WT at 2 months (**Fig 1C**), providing the first hint of an
182 acceleration of the ageing transcriptomic profile in the *tert*^{-/-}. We found that there was
183 higher variability in the gut than in the brain, between samples within each age group (**Fig**
184 **1C and D**). A summary of the number of significant differentially expressed genes (DEGs) in
185 all samples is represented in **Fig. 1E**. How these DEGs relate to which other, how many

186 overlap and how many are in common or accelerated in the absence of telomerase (*tert*^{-/-}),
187 will be explored later in the manuscript.

188 To identify genes and pathways that are consistently up- or down-regulated in a time-
189 dependent manner in natural ageing in the zebrafish gut and brain, we grouped the genes
190 into temporal expression profiles, by time-series analysis using Short Time-series Expression
191 Miner (STEM) software (Ernst & Bar-Joseph, 2006). To determine whether the temporal
192 profiles were associated with specific biological processes and pathways, pathway over-
193 representation analysis (ORA) were performed for the genes assigned to the significant
194 STEM profiles. Enrichments of GO Biological Process (GOBP), GO Molecular Function
195 (GOMF), GO Cellular Compartment (GOCC), Kyoto Encyclopedia of Genes and Genomes
196 (KEGG) terms and REACTOME pathway terms were therefore analysed for each profile.
197 Time-series analysis of WT gut identified 9 different profiles, with 2 of them containing up-
198 regulated genes (profiles 7 and 21. Total of 523 genes), and 7 containing down-regulated
199 genes (profiles 32, 31, 23, 9, 12, 22 and 34. Total of 11,594 genes) (**Fig. 2A1 and source**
200 **data**). Interestingly, in the *tert*^{-/-} gut, all the profiles identified by time-series analysis contain
201 up-regulated genes (profiles 8, 6, 15 13, 12 and 11. Total of 10,317 genes) (**Fig. 2A2 and**
202 **source data**). Enrichment analysis showed that the profiles containing up-regulated genes
203 are associated with immune response, while profiles containing down-regulated genes are
204 largely associated with proliferation, cellular response to DNA damage, and DNA damage
205 repair, in both WT and *tert*^{-/-} gut (**Fig. 2 A1.1, 1.2 and A2.1**). To help contextualise our
206 analysis, we performed a further classification of enriched processes according to the
207 hallmarks of ageing, which have been previously identified (Lemoine, 2021; López-Otín et
208 al., 2013). This classification further strengthened the observation that the up-regulated
209 profiles include genes mostly involved in altered intercellular communication, in which
210 immunity and inflammation play a key role, whereas the down-regulated profiles identify
211 stem cell exhaustion and genomic instability as the main hallmarks of ageing, to which the
212 genes affecting proliferation, DNA damage and repair are likely to contribute (**Fig. 2 A1.1,**
213 **1.2 and A2.1 and source data**).

214 In the WT brain, we identified 9 temporal profiles, 6 of them including up-regulated
215 genes (profiles 42, 29, 40, 30, 21 and 48. Total of 7,230 genes), and 3 including down-
216 regulated genes (profiles 1, 12 and 26. Total of 561 genes) (**Fig. 2B1 and source data**). In the

217 *tert*^{-/-} brain, time-series analysis revealed 6 different profiles. Profiles 4, 0 and 3 containing
218 down-regulated genes (total of 5,374 genes) and profiles 15, 12 and 11 containing up-
219 regulated genes (total of 1,155 genes) (**Fig. 2B2 and source data**). As in the gut, up-
220 regulated profiles reveal genes mostly involved in immune regulation and inflammation and
221 down-regulated profiles are mostly involved in cell cycle, genome stability and DNA damage
222 responses, in both genotypes This is further highlighted when placed into context by the
223 analysis based on the hallmarks of ageing, where up-regulated profiles identify altered
224 intercellular communication whereas the down-regulated ones identify stem cell exhaustion
225 as the main hallmarks affected (**Fig 2 B1.1, 1.2; B2.1, 2.22 and source data**).

226 In summary, STEM analysis and enrichment pathways in both gut and brain ageing
227 show a general trend towards up-regulation of genes involved in immune response and
228 down-regulation of genes involved in cell cycle, DNA damage and repair. This general trend
229 is recapitulated in the absence of telomerase. These mechanisms are all known contributors
230 to the well-described altered intercellular communication, genome stability and stem cell
231 exhaustion hallmarks of ageing, respectively (Lemoine, 2021; López-Otín et al., 2013).

232

233 **2.2 Comparing the hallmarks of ageing over time, in WT and *tert*^{-/-} zebrafish gut and** 234 **brain**

235 More than just identifying the signatures of natural WT ageing in the gut and brain
236 and identifying telomerase-dependent and -independent changes, we wanted to
237 understand if there were particular changes occurring before others, and how their kinetics
238 compared between the gut and the brain. In order to contextualise our analysis in the light
239 of the well-described hallmarks of ageing, (Lemoine, 2021; López-Otín et al., 2013), we used
240 the main hallmarks of ageing as headers in which we could group the different changes in
241 processes that were enriched from both the STEM profiles and all DEGs. This allowed us to
242 compare the effects of age, genotype and tissue on the evolution of the key hallmarks of
243 ageing. When we combine all the gene changes (up- and down-regulated) and associated
244 biological processes affected (**Fig. 3 and source data**), we observe distinct tissue-specific
245 signatures of ageing, namely in the gut (**Fig. 3A**) and brain (**Fig. 3B**), particularly when
246 considering the time-series analysis on its own (STEM) (**Fig 3. A1 and B1**). Whereas ageing in
247 the WT gut seems to be predominantly affected by the de-regulated nutrient sensing

248 initially, the brain displays stem cell exhaustion as the main hallmark affected at the early
249 age of 9 months (**Fig. 3A1, B1**, respectively). When we combine the different analysis,
250 though (**Fig. 3A3 and B3**), both gut and brain have stem cell loss as the main hallmark of
251 ageing associated with the enriched processes found at 9 months of age, highlighting this as
252 a potential contributor to the early stages of ageing in both tissues. Towards the end of life,
253 both gut and brain have altered intercellular communication as the main hallmark of ageing
254 identified. Importantly, independently of the analysis, the *tert*^{-/-} zebrafish show accelerated
255 hallmarks of ageing. In specific, a *tert*^{-/-} 2-month-old gut profile is very similar to a WT 35 gut
256 month profile (**Fig. 3A**). In the brain, at 2 months of age the *tert*^{-/-} mutant also displays some
257 of the hallmarks of ageing that also become altered in WT ageing at later ages, particularly
258 altered intercellular communication, but the *tert*^{-/-} brain becomes much more similar to the
259 aged WT from the age of 9 months onwards (**Fig. 3B**). This suggests that hallmarks of ageing
260 accelerated in the absence of telomerase are developing earlier in the gut than in the brain.

261 Finally, when we look at the overall number of gene expression changes, i.e, not just
262 the ones associated with the hallmarks of ageing, we observe that there is a general
263 increase in the number of changes in gene expression with ageing (**Fig 3 A4 and B4**).
264 However, this increase does not appear to be linear. In specific, in the gut, the number of
265 DEGs is fairly low until 9 months of age, after which there seems to be an inflexion point and
266 the number of DEGs increases up to 5-fold in the oldest WT (>35 months) and 3 fold in the
267 oldest *tert*^{-/-} (22 months). In the brain, there seems to be a more gradual, consistent
268 increase over time, both in WT and *tert*^{-/-}. This increase in number of DEGs with ageing may
269 be a consequence of the known de-regulation of gene expression with ageing due to de-
270 repression of heterochromatin and/or changes in epigenetic markers.

271

272 **2.3 When does a *tert*^{-/-} resemble an aged WT the most?**

273 It is of note that, even though the *tert*^{-/-} accelerates hallmarks of ageing in the gut and
274 brain, the set of genes identified are not necessarily the same as in WT ageing. In specific,
275 looking at the genes at the early stages of ageing, the most significant hallmark of ageing
276 shared between the 2 months old *tert*^{-/-} and WT 9 months gut is nutrient sensing, and only 2
277 up-regulated genes are in common, namely *lipca* (*Hepatic triacylglycerol lipase precursor*)
278 and *pla1a* (*phospholipase 1a*). Interestingly, hepatic lipase has been involved in

279 atherogenesis (Santamarina-Fojo, Gonzalez-Navarro, Freeman, Wagner, & Nong, 2004), and
280 age-related macular degeneration (Neale et al., 2010), diseases that have been
281 hypothesised to have a parallel response to tissue injury induced by multiple factors,
282 including impaired immune responses, and oxidative stress (Neale et al., 2010). In line with
283 the general de-regulated inflammatory response we see in the gut, with ageing (**Figs. 2 and**
284 **3 and source data**), *phospholipase 1a* has been reported to be up-regulated in inflamed gut
285 tissue of Crohn's disease patients (Hong et al., 2017) and has a complex role in the
286 regulation of immunity and inflammation (recently reviewed in (Zhao, Hasse, & Bourgoin,
287 2021)). In the brain, there are no genes in common between the 2 months old *tert*^{-/-} and WT
288 9 months associated with altered intercellular communication or genomic instability, the 2
289 main hallmarks of ageing shared between the genotypes at the early stages of ageing.
290 Following this type of analysis, we could then ask at what age does the *tert*^{-/-} best mimic
291 naturally aged WT, at the level of gene expression from the shared hallmarks of ageing and
292 these "other" genes we found to be associated with ageing but not obviously associated
293 with the described hallmarks of ageing. We therefore analysed the overlap between all
294 DEGs identified in the old WT (35 months) and the *tert*^{-/-} at the different aged (2, 9 and 22
295 months), using Venn diagrams created using the Venny 2.1 online platform (Oliveros, 2007-
296 2015) to ask this question. We observe that the 2 months old *tert*^{-/-} has the most genes
297 shared with the 35 months old WT gut (59 genes in common) (**Fig. 4 A1 and Supp. Fig. 1**)
298 whereas it is the *tert*^{-/-} at 22 months that has the most genes shared with the 35 months old
299 brain (112 genes in common) (**Fig. 4 B1 and Supp. Fig.1**). This similarity between the 2
300 month and 22 months *tert*^{-/-}, with the gut and brain, respectively, is also apparent when we
301 just look at the pattern of the main hallmarks of ageing accelerated in the *tert*^{-/-} (**Fig. 3, 4**
302 **and Graphical Abstract**). Together, these data suggest that the gut is displaying telomerase-
303 dependent hallmarks of ageing at an earlier age than the brain, consistent with what would
304 be expected for a high *versus* low proliferative tissue. Of relevance, In the brain, of the
305 genes de-regulated in the *tert*^{-/-} 22 month that are in common with the WT aged at 35
306 months *ccna2* (cyclin a2), *cdk6* (cyclin-dependent kinase 6), *chek1* (checkpoint kinase 1),
307 *mad2l1* (Mitotic spindle assembly checkpoint protein mad2a), *tacc3* (Transforming, acidic
308 coiled-coil containing protein 3), *top2a* (DNA topoisomerase ii alpha) and *mcm2* (DNA
309 helicase, *MCM2 minichromosome maintenance deficient 2*) have also been included in the
310 Human Ageing Resources databases (Tacutu et al., 2018) and are mostly located within the

311 same cluster (green), identified using *k-means* clustering in STRING analysis (Szkarczyk et
312 al., 2021) (**Fig 4 and source data**). Of the proteins encoded by these genes, *chek1*
313 (Poehlmann et al., 2011), *cdk6* (Morris, Hepburn, & Wynford-Thomas, 2002), *mad2l1*
314 (Lentini, Barra, Schillaci, & Di Leonardo, 2012), *tacc3* (Schmidt et al., 2010) have been
315 reported to be involved in cellular senescence, . Additionally, *Top2a* has also been involved
316 in neuron proliferation (Watt & Hickson, 1994) and *mcm2* depletion in mice leads to
317 decreased proliferation in various tissue stem cell progenitors (Pruitt, Bailey, & Freeland,
318 2007).

319

320 **2.4 Analysis of telomerase (*tert*)-dependent gene changes of old age**

321 Once we identified what WT ageing looked like at the level of time-dependent gene
322 expression changes over the life-course and the main biological processes affected, we
323 sought to determine how much of these were likely to be telomerase-dependent. If a gene
324 expression change or a biological process alteration is accelerated in the absence of
325 telomerase (i.e becomes significant at an earlier age in the *tert*^{-/-}), we consider it to be
326 telomerase dependent, as has been described before (Madalena C Carneiro et al., 2016;
327 Henriques et al., 2013). Conversely, if none of these pre-requisites are met, we consider the
328 gene/process alteration to be telomerase-independent. With this in mind we performed
329 Venn diagrams (Oliveros, 2007-2015) to identify the telomerase-dependent significant gene
330 alterations of old age, i.e, DEGs present in the WT at 35months old, when compared with
331 the WT young control. For this, we used the DEGs identified in the STEM profiles (i.e., genes
332 that change monotonically, in a time-dependent manner), combined with the more
333 traditional DEG analysis, which include all gene changes, whether they change consistently
334 in a time-dependent manner across the lifecourse or not (called “all DEGs” from hereafter)
335 (**Fig. 5 and source data**). From these analyses, we identified 50 significant DEGs (out of 491;
336 c. 10%) (present in old age (WT 35 months) that are prematurely de-regulated in the *tert*^{-/-}
337 gut (**Fig. 5 A**) and 100 genes (out of 428; c.23%) to be prematurely de-regulated in the *tert*^{-/-}
338 brain (**Fig. 5 B**). Importantly, most of these genes are directly or indirectly involved in known
339 hallmarks of ageing (Lemoine, 2021; López-Otín et al., 2013), namely altered intercellular
340 communication (including immunity, inflammation, extra-cellular matrix), genome stability
341 (including DNA replication and repair), stem cell exhaustion and mitochondrial dysfunction,

342 as was also evident in **Fig 3** and now further detailed below. In the gut, telomerase-
343 dependent gene expression changes with ageing include up-regulation of genes involved in
344 immune response, such as *tlr18* (*Toll-like receptor 18 precursor*), *syt11* (*Synaptotagmin-like*
345 *protein 1*) and down-regulation of genes involved in metabolism, such as *cyp8b1* (*Bertaggia*
346 *et al., 2017*) (*Cytochrome P450, family 8, subfamily B, polypeptide 1*) and *igfbp2a* (*Insulin-*
347 *like growth factor-binding protein 2*). Within the down-regulated genes, there are other
348 well-known genes such as *sox6* (involved in stem cell function), *vav3b* (involved in wound
349 healing), (**Fig 5 and source data**). Additionally, we identify a number of non-annotated
350 genes, which may represent novel *tert*-dependent genes, that would require further
351 investigation. Importantly, amongst these *tert*-dependent genes of “old age”, there are a
352 number of homolog or closely related genes which have been previously identified in ageing
353 datasets (Tacutu et al., 2018) such as several *igfbps* (*insulin-like growth factor binding*
354 *proteins*), *igf* (*insulin growth factor*), *mapks* (*mitogen-activated protein kinases*), *tlr3* (*toll-*
355 *like receptor 3*) and *nrg1* (*neuregulin 1*).

356 In the brain, *tert*-dependent ageing gene expression changes include mostly down-
357 regulation of genes involved in cell cycle or neurogenesis, such as *aurkb* (*aurora kinase B*),
358 *chek1* (*checkpoint kinase 1*), *ccnb1* (*cyclin b1*), *cdk2* (*cyclin-dependent kinase 2*) and *neurod4*
359 (*neuronal differentiation 4*), *dld* (*delta d*), *nog1* (*noggin 1*), respectively, as well as genome
360 stability and DNA repair, such as *rad54l* (*rad54 like*), *mcm5* (*minichromosome maintenance*
361 *complex component 5*) and *smc4* (*structural maintenance of chromosomes 4*). Up-regulated
362 genes are mostly involved in immune response or inflammation, such as *cxcl18b* (*chemokine*
363 *(C-X-C motif) ligand 18b*), *mhc2a* (*major histocompatibility complex class II integral*
364 *membrane alpha chain gene*), *socs1a* (*suppressor of cytokine signaling 1a*), *irf8* (*interferon*
365 *regulatory factor 8*) and *csf1b* (*colony stimulating factor 1b (macrophage)*). Of note,
366 amongst these *tert*-dependent DEGs of old age, we identified *dre-mir-29b-1*, which encodes
367 for a regulatory micro RNA 29 (mir29), widely described to be up-regulated in ageing, in
368 response to DNA damage, alongside P53 (Ugalde et al., 2011) and can act as a protective
369 response, limiting excessive iron-exposure and damage in neurons (Ripa et al., 2017). As for
370 the gut, there are a number of homolog or closely related genes which have been previously
371 identified in ageing (Tacutu et al., 2018), such as *chek1*, *mad2l1* (*MAD2 mitotic arrest*
372 *deficient-like 1 (yeast)*), *dl3* (*delta like 3*), *nog* (*noggin*), *ifnb1* (*interferon beta*), *socs2*

373 (*suppressor of cytokine signaling 2*), amongst many others, which can be found in the
374 GeneAge database.

375 Since it is known that short telomeres themselves can lead to de-regulated gene
376 expression, particularly in genes near the chromosome ends due to loss of the “telomere
377 positioning effect” (TPE) (Robin et al., 2014), we proceeded to map the genes identified to
378 be de-regulated prematurely in the absence of telomerase to their chromosome location,
379 with the aim of determining whether they located to within up to 10MB of either of the
380 telomeric ends (**Fig. 5C1**). We found that whereas most *tert*-dependent gene changes of old
381 age do not locate to the end of chromosomes, in both gut and brain (**Fig. 5C2 and C3**).
382 However, there are significantly more *tert*-dependent genes located at the end of
383 chromosome in the gut than in the brain, (**Fig. 5 C4**). This is consistent with gut being a more
384 proliferative tissue, where telomeres are likely to shorten more, which would be particularly
385 exacerbated in the absence of *tert*, leading to a higher probability of TPE contributing to
386 gene transcription alterations.

387 **2.5 Transcriptional changes in common between the gut and brain at the early and** 388 **late stages of ageing**

389 Even though the aged phenotype is something usually observed late in life, the
390 underlying molecular and cellular mechanism driving these changes can, arguably, start
391 from the moment you are born (Gladyshev, 2021). To understand what significant
392 transcriptional changes are taking place in the gut and brain and, in particular, in common
393 between the gut and brain, we compared all DEGs and STEM DEGs in these tissues at the
394 earliest time point we detect significant changes (9 months) and at the late stages of ageing,
395 i.e, at the latest time point analysed of 35 months (**Fig 6, Supp Fig 3 and source data**). We
396 identified 7 gene changes in common between WT gut and brain at the early stages of
397 ageing (9 months of age). In specific, we identified 5 down-regulated genes, namely *ccnb1*,
398 *kif2c*, *serpinh1a*, *temem37* and *si:ch211-5k11.8*, and 2 up-regulated genes, namely *cfap45*
399 and *eif4ebp3l*. Of these, *ccnb1* (*G2/mitotic-specific cyclin-B1*) and *kif2c* (*Kinesin-like protein*)
400 are both proteins involved in cell-cycle progression. Whereas *Ccnb1* has been reported to be
401 involved in normal stem-cell/progenitor maintenance in the brain (Hagey et al., 2020) and
402 gut (Basak et al., 2014); *kif2c* can act as a DNA damage repair protein, and, accordingly, its
403 depletion leads to significant accumulation of DNA damage (Zhu et al., 2020). STRING

404 analysis suggests these proteins are likely to be co-expressed in a variety of organisms
405 including zebrafish and humans, highlighting potential functional links (**Fig 6 B and source**
406 **data**). The downregulated *elf4ebp3l* gene (Eukaryotic translation initiation factor 4E-binding
407 protein 3-like) encodes a repressor of translation and is inhibited in response to TORC1
408 (mammalian target of rapamycin complex 1) (Boutouja, Stiehm, & Platta, 2019).

409 At “late stages” of ageing, we identified 23 gene changes in common between the gut
410 and brain. Of these, STRING analysis identified 2 main protein network interactions, namely
411 a link between cd59 and cd99l2 and link between il2rb and b2m. In specific, cd59 and cd99l,
412 which our data show to be downregulated in old age, in both gut and brain, have both been
413 cited in the literature as markers of new-born neurons and oligodendrocyte progenitor cells,
414 respectively, in a single-cell transcriptomic analysis of the adult zebrafish brain (Lange et al.,
415 2020). In the gut, cd59, also known as protectin, has been shown to be downregulated in
416 the gut epithelium of ulcerative colitis and Chron’s disease patients and thought to render
417 the tissue susceptible to inflammatory damage (Scheinin et al., 1999). cd99 has been shown
418 to be a key molecule in modulating monocyte migration through endothelial junctions
419 (Schenkel, Mamdouh, Chen, Liebman, & Muller, 2002) and monocyte differentiation to
420 macrophages is known to be triggered by endothelial transmigration (Gerhardt & Ley, 2015;
421 Li et al., 2020), including in the brain via migration through the blood-brain barrier (Ifergan
422 et al., 2007). Il2rb and b2m, which our data show to be up-regulated in both gut and brain at
423 the “late stages” of ageing, are key molecules involved in adaptive and innate immune
424 function. Whilst the IL2R beta is important for T-cell mitogenic response to IL-2, the b2m
425 (Beta-2-microglobulin) protein is a component of the major histocompatibility complex I
426 (MHCI), involved in antigen presentation. Intriguingly, b2m has been shown to be present in
427 a soluble free-form, and has been found to be systemically increased with ageing in humans
428 and in individuals with neurodegenerative diseases (Smith et al., 2015). Importantly,
429 heterochronic parabiosis experiments between young and old mice suggest that increased
430 b2m with ageing leads to cognitive impairment and neurodegeneration, and has hence been
431 identified as a systemic pro-ageing factor (Smith et al., 2015). Additionally, increased IL2
432 receptor expression has been shown to contribute to CD4 differentiation and exhaustion of
433 their naïve pool and therefore ability to respond to infection with ageing, in humans
434 (Pekalski et al., 2013; H. Zhang, Weyand, & Goronzy, 2021).

435

436 **3 DISCUSSION**

437 In this study, we used RNA sequencing analysis to determine the kinetics of
438 telomerase-dependent and -independent transcriptomic changes occurring during WT
439 ageing in brain and gut tissues, using the zebrafish as a model. We hypothesised that this
440 would allow us to identify key age-associated genes and pathways that become prematurely
441 de-regulated in both or either tissue, providing key insights into the early stages of ageing in
442 each tissue and highlight potential interactions.

443

444 **3.1 STEM versus all DEGs analysis**

445 Ageing can be described as a time-dependent change in tissue homeostasis, that
446 increases the probability of disease and death (Hayflick, 2007). Whether the genes and
447 pathways driving these time-dependent changes are also consistently changing in a time-
448 specific manner, remains unresolved. To account for both possibilities, we performed a
449 time-series analysis (STEM) and then combined this with the more traditional differential
450 gene expression (DEGs) analysis between young and old animals. Even though the gene
451 changes identified with the STEM analysis were also picked up by the traditional DEGs
452 analysis, the STEM analysis provided a much tighter, restrictive view of the transcriptomic
453 signatures of ageing. In the gut, particularly, the main hallmarks of ageing identified using
454 the STEM analysis are quite different from the ones using the traditional all DEGs. In
455 particular, STEM analysis identifies mitochondrial dysfunction and de-regulated nutrient
456 sensing as the main hallmarks of WT ageing at the earlier stages of ageing in the gut (WT 9
457 months), whereas all DEGs analysis identified stem cell dysfunction as the principal hallmark
458 de-regulated at that age. The significance of these differences is difficult to judge, but it can
459 suggest that changes in genes affecting mitochondrial function and nutrient sensing have a
460 mostly monotonic trajectory in gut ageing, whereas the ones involved in stem cell
461 maintenance can have different behaviours at different times throughout life. Nevertheless,
462 this difference was not observed in the WT brain or in the *tert*^{-/-} ageing, where STEM and all
463 DEGs analysis led to very similar conclusions regarding the identity or kinetics of the main
464 hallmarks of ageing affected. Importantly, the kinetics of gene changes and processes
465 identified in our data match very well to the phenotypes of ageing previously reported in
466 the *tert*^{-/-} and WT ageing. In particular, in the gut, impaired cell proliferation in the gut is one

467 of the first *tert*-dependent phenotypes of ageing identified, followed by cellular senescence
468 and inflammation later in life (Madalena C Carneiro et al., 2016; Henriques et al., 2013).
469 Moreover, the recently reported *tert*-dependent changes in macrophage immune activation
470 and increased gut permeability (Pam S. Ellis, 2022) are consistent with key *tert*-dependent
471 gene changes of old age identified here. An example of such genes are *cd99*, potentially
472 involved in macrophage differentiation via trans-endothelial migration (Gerhardt & Ley,
473 2015; Li et al., 2020; Schenkel et al., 2002); and *cldn5a* (claudin 5), involved in tight-junctions
474 (Lu, Ding, Lu, & Chen, 2013).

475

476 **3.2 Main hallmarks of ageing**

477 A simplistic prediction of how the kinetics of the hallmarks of ageing would behave
478 over the lifecourse could be that, at early ages, we would detect more changes affecting the
479 primary hallmarks of ageing, i.e. the “causes of damage”, namely genomic instability,
480 telomere attrition, epigenetic alterations and loss of proteostasis. At the last stages, one
481 could predict that we would detect more significant changes in the integrative hallmarks,
482 i.e. the “culprits of the phenotype”, namely stem cell exhaustion and altered intercellular
483 communication, of which inflammation is a key component, as described in (López-Otín et
484 al., 2013). However, either separately or combined, neither STEM nor all DEGs analysis show
485 this. Our combined analyses show that most of the gene changes occurring at the early
486 stages of WT ageing are observed from 9 months and are mostly involved in stem cell
487 maintenance, in both gut and brain. One potential explanation for this observation, is that
488 our qualitative analysis was not able to distinguish between such hallmarks or is under-
489 estimating the primary hallmarks. Another explanation comes from the relatively low
490 sample size used for each time-point and the heterogeneity of individuals physiology
491 amongst each population. As recently showed in (Dambrose et al., 2016), zebrafish age
492 following the two-phase model first proposed flies (Tricoire & Rera, 2015), based on the
493 age-related intestinal permeability assessed using the Smurf assay they previously described
494 (Rera, Clark, & Walker, 2012). Moreover, we have recently shown that gut permeability with
495 ageing is accelerated in the absence of telomerase (*tert*^{-/-}) (Pam S. Ellis, 2022). Following this
496 model and considering the longevity curve from the population we sampled, the proportion
497 of Smurfs might have been approximately, <10% at 2 month, 25% at 9 month, 50% at 22

498 months and >80% at 35 months. The chances to have selected at least 1 Smurf by accident
499 are approximately 27% at 2 months, 57% at 9, 86% at 22 and 99% at 35%. This could
500 contribute to the heterogeneity or potential bias towards having more of a specific ageing
501 signature over another (smurf versus non-smiurf).

502 At first glance, it is surprising that telomere dysfunction is not picked up as a main
503 hallmark of ageing in the telomerase mutant model. However, this may simply be the
504 reflection of the number of genes that have been directly implicated in each of these
505 hallmarks. In specific, there are a lot less genes that one would identify as directly involved
506 in telomere dysfunction, when compared to stem cell dysfunction, for example. The main
507 culprits for telomere dysfunction would be telomerase and the shelterin components,
508 whereas for stem cell dysfunction, all the cell cycle and DNA damage repair proteins can
509 play a role. For example, *chek1*, *fxr1* and *daxx*, which are all de-regulated in the old WT gut
510 and brain (*chek1*) (see source data), have all been identified as potential regulators of
511 telomeres (Nersisyan et al., 2019). Yet, because that is not the main function one would
512 attribute to such genes, these would have been missed as part of the telomere dysfunction
513 hallmark of ageing. Additionally, it is not possible to distinguish from just looking at lists of
514 DEGs if such gene was de-regulated due to telomere dysfunction in the first place, or if its
515 dysfunction will affect telomere function indirectly. These are some of the considerations
516 that highlight the complexity of ageing and the non-linearity of how the hallmarks of ageing
517 may drive ageing as well as each other and it is important to have them in mind when
518 interpreting our analyses. Nevertheless, at the later stages of WT ageing (>35 months),
519 altered intercellular communication, a previously described “culprit of the phenotype” is
520 indeed the most significant hallmark of ageing detected in common between the gut and
521 brain. Finally, in terms of the progression hallmarks of ageing, different hallmarks may play
522 more prominent roles at specific times of life, and may be replaced by others at other times,
523 explaining why we don’t necessarily always see a linear accumulation of the different
524 hallmarks of ageing over-time. This is particularly evident in the gut, where stem cell
525 exhaustion is the main hallmark identified by the combined STEM and ALL DEGs analysis,
526 and it is barely represented at the later stages of life. In the brain, the progression seems to
527 be more linear, though, and most hallmarks present at the early time point of 9 months
528 remain until old age, when other hallmarks are further added.

529

530 **3.3 Telomerase- and/or telomere-dependent changes with ageing**

531 If a gene expression changes or a biological process alteration is accelerated in the
532 absence of telomerase (i.e becomes significant at an earlier age in the *tert*^{-/-}), we considered
533 it to be telomerase dependent. If we take a step back and look at the processes and, in turn,
534 hallmarks of ageing affected in the absence of telomerase, it becomes clear that the *tert*^{-/-} is
535 indeed accelerating many of these changes. It is particularly evident when we look at the pie
536 charts depicting the different hallmarks of ageing affected at each time point in WT versus
537 *tert*^{-/-}. Here, it is striking how a 2-month-old *tert*^{-/-} gut resembles a WT gut at the old age of
538 35 months, and how a 9- and 22-month-old *tert*^{-/-} brain resembles an old WT brain at 35
539 months. This is further highlighted by the further comparison we performed, where we
540 asked at which age does the *tert*^{-/-} share more gene expression changes with the WT old
541 (>35 months). In this analysis, we show that the 2 months old *tert*^{-/-} has the most gene
542 expression changes shared with the 35 months old WT gut, whereas it is the *tert*^{-/-} at 22
543 months that has the most gene expression changes shared with the 35 months old WT
544 brain. This suggests that the gut is displaying telomerase-dependent hallmarks of ageing at
545 an earlier age than the brain, which is consistent with what would be expected for a high
546 versus low proliferative tissue. Accordingly, when looking at the specific gene changes
547 accelerated in the absence of *tert*, i.e, we identify significantly more *tert*-dependent genes
548 located near the ends of chromosomes in the gut than in the brain, and therefore more
549 liable to have been altered due to telomere shortening. In the future, it would be insightful
550 to test how many of the *tert*-dependent gene changes occur due to non-canonical functions
551 of telomerase involved in transcriptional regulation.

552 Nevertheless, *tert*-dependent gene changes in both tissues are still a minority, serving
553 as a reminder that “all roads lead to Rome”, and one should exercise caution when trying to
554 identify genes influencing the natural process of ageing using premature ageing models. It is
555 not necessarily the same genes influencing the processes of ageing in these models, even if
556 the processes and phenotypes are accelerated. We should also have this in mind when we
557 compare the sets of genes identified in this study with those previously identified as
558 implicated in human ageing, and not necessarily be surprised if only a small percentage of
559 those are shared. One could argue that it is more important that the processes are shared.

560 Nevertheless, we do identify many gene changes shared between zebrafish and human
561 ageing databases as highlighted throughout the results' section.

562 **3.4 Which genes to focus on if we were to target age-associated dysfunction in the** 563 **gut and brain.**

564 As a final step in our analysis, we wanted to identify common gene expression
565 changes between the gut and the brain at the earliest stages of ageing, in our case, from the
566 age of 9 months. We hypothesised that this may highlight potential common therapeutic
567 targets for early intervention to prevent age-associated dysfunction in both tissues. We
568 identified 8 significant DEGs in common between the gut and brain at 9 months of age, 5
569 down-regulated (*ccnb1*, *kif2c*, *serpinh1a*, *si:ch211-5k11.8* and *tmem37*) and 2 up-regulated
570 (*cfap45* and *EIF4EBP3*). We could then hypothesise that restoring expression of these genes
571 to youthful levels would have a positive impact on delaying or ameliorating the
572 development of ageing phenotypes in both these tissues at the same time. Of note, we
573 identified that, amongst these, *ccnb1* and *EIF4EBP3* were telomerase-dependent changes in
574 the brain. If so, one could hypothesise that telomerase re-activation in the brain should
575 restore these genes to young WT levels and potentially contribute to amelioration of *ccnb1*-
576 and *EIF4EBP3*-dependent ageing phenotypes in the brain.

577

578 **4 CONCLUSIONS**

579 We provide the first systematic analysis of transcriptomic changes throughout the
580 lifespan of zebrafish in the gut and brain of the same group of individuals, leading to the
581 identification of key genes and processes likely involved in driving the ageing process in
582 these tissues. Many of these genes have previously identified in human ageing databases
583 and many of them are potentially new genes of ageing, which will have to be experimentally
584 tested in relevant model organisms. This analysis and the open access availability of its
585 source and raw data should provide a key steppingstone and framework supporting future
586 work for understanding the ageing process and using zebrafish for studying ageing.

587

588 **5 MATERIALS AND METHODS**

589 **5.1 Zebrafish husbandry, genotypes and ages**

590 Zebrafish were maintained at the standard conditions of 27-28°C, in a 14:10 hour
591 light-dark cycle, and fed twice a day with *Artemia* (live rotifers) and Sparus (dry food). All
592 the experiments were performed in the University of Sheffield. All animal work was
593 approved by local animal review boards, including the Local Ethical Review Committee at
594 the University of Sheffield (performed according to the protocols of Project Licence
595 70/8681).

596 Two strains of adult zebrafish (*Danio rerio*) were used for these studies: wild-type
597 (WT; AB strain) and *tert*^{-/-} (*tert*^{AB/hu3430}). Wild-type fish were obtained from the Zebrafish
598 International Resource Center (ZIRC). The *telomerase* mutant line *tert*^{AB/hu3430} was generated
599 by *N*-ethyl-nitrosourea mutagenesis (Utrecht University, Netherlands (Wienholds et al.,
600 2003)). It has a T→A point mutation in the *tert* gene and is available at the ZFIN repository,
601 ZFIN ID: ZDB-GENO-100412-50, from ZIRC. The fish used in this study are direct descendants
602 of the ones used previously^{29,30}, by which point it had been subsequently outcrossed five
603 times with WT AB for clearing of potential background mutations derived from the random
604 ENU mutagenesis from which this line was originated. The *tert*^{hu3430/hu3430} homozygous
605 mutant is referred to in the paper as *tert*^{-/-} and was obtained by incrossing
606 our *tert*^{AB/hu3430} strain. Genotyping was performed by PCR of the *tert* gene^{13,14}. In order to
607 study age-related phenotypes in the zebrafish gut and brain, we used >30 months old fish
608 for what we consider old in WT (in the last 25-30% of their lifespan), and we considered the
609 *tert*^{-/-} old fish at the equivalent age (>22 months), which approximately corresponds to the
610 last 25-30% of their lifespan. In specific, 'Old' was defined as the age at which the majority
611 of the fish present age-associated phenotypes, such as cachexia, loss of body mass and
612 curvature of the spine. These phenotypes develop close to the time of death and are
613 observed at >30 months of age in WT and at >22 months in *tert*^{-/-} (Madalena C Carneiro et
614 al., 2016; Henriques et al., 2013).

615

616 **5.2 Tissue dissection and RNA extraction**

617 Animals from various age-groups were used for RNA-Sequencing (WT at 2, 9, 22 and
618 >30 months of age; and *tert*^{-/-} at 2, 9 and 22 months of age). Three biological replicates were
619 used per group. Fish were culled by overdose of MS-222, followed by confirmation of death.
620 Then, the whole tissues were rapidly dissected in cold PBS (Sigma-Aldrich), transferred to a

621 microcentrifuge tube containing 100 μ l of Trizol (Thermo Fisher Scientific), snap-frozen in
622 dry ice and stored at -80° . To isolate the RNA, extra 50 μ l of Trizol was added to each
623 sample, and the tissue was homogenized with a mechanical homogenizer (VWR
624 International) and a 1.5 pestle (Kimble Chase, Vineland, NJ, USA). After 5 min incubation at
625 room temperature (RT), 30 μ l of chloroform (1:5, VWR International) was added and the
626 samples were incubated for further 3 min at RT before centrifuged at 13,000g, for 30 min, at
627 4° C. Isopropanol (Thermo Fisher Scientific) was then added to the aqueous phase of the
628 solution, and the resultant mix was incubated for 10 min at RT, before centrifuged (13,000g
629 for 15 min at 4° C). Finally, the pellet was twice washed in 250 μ l of ice cold 75% ethanol and
630 left to air-dry, before resuspended in 14 μ l of nuclease-free water. RNA integrity was
631 assessed with the bioanalyzer Agilent 2100 Bioanalyzer (Agilent, Santa Clara, CA, USA). All
632 the samples had a RNA integrity number (RIN) ≥ 9 .

633

634 **5.3 RNA-Sequencing**

635 The RNA-Sequencing was performed at the *Genomics and Sequencing facility* of
636 Sheffield Institute for Translational Neuroscience (SiTraN). Library preparation was
637 performed following the Illumina methodology. mRNA was extracted from 500 ng of RNA
638 with oligo-dT beads, capturing poly(A) tails, using the NEBNext Poly(A) mRNA Magnetic
639 Isolation Module (New England Biolabs Inc). cDNA libraries were made with the NEBNext[®]
640 Ultra™ RNA Library Prep Kit for Illumina, following the manufacturer's instructions (New
641 England Biolabs Inc). The samples were then sequenced on an Illumina HiSeq SQ, using a
642 high output run and sequencing by synthesis V3 chemistry on a single 100 bp run. The data
643 was imported into a FASTQ file format in order to perform the analysis.

644

645 **5.4 RNA-Sequencing analysis**

646 **5.4.1 Data processing.** Quality control was performed using MultiQC version 1.9.
647 Cutadapt version 3.0 was used for trimming the first 13 bases from the reads to remove
648 poor quality base pairs in the reads. Read alignment was performed as follows. Single-end
649 reads were aligned against the reference genome *Danio rerio*.GRCz11.dna.
650 primary_assembly.fa using STAR. A bespoke alignment index was built using annotation file

651 Danio_erio.GRCz11.103.gtf and an expected read length of 88 bp. Ht-seq count was run in
652 non-stranded mode to obtain *per gene* read counts.

653 **5.4.2 Differential expression.** To identify signatures of ageing, WT gut and brain
654 samples were subjected separately to DESeq2 analysis, comparing the time points 9, 22 and
655 >30 months with the time-point of 2 months. Then, *tert*^{-/-} samples at 2, 9 and 22 months
656 were contrasted with WT at 2 months, in order to identify telomerase-dependent ageing
657 processes.

658 **5.4.3 Time-series analysis.** Short Time-series Expression Miner (STEM) software was
659 used to assign genes to predefined expression profiles genes based on their expression
660 across the time points. For this, the 2 months' time-point was used as the zero time point
661 for the analysis. The maximum number of model profiles was set to 50; the maximum unit
662 change in model profiles between time points was set to 2; and the minimum absolute log
663 ratio of expression was set to 1.0, with change based on maximum – minimum. Significance
664 level of the model profiles was set to 0.05 with Bonferroni correction. Minimum correlation
665 for profile clustering was set to 0.7. The statistically significant temporal profiles were
666 visualised as line plots using ggplot2. Median expression fold change values of the genes in
667 each profile were shown on the plots with a thicker line.

668 **5.4.4 Enrichment analysis of temporal profiles from STEM.** Enrichment analysis was
669 performed using all the differentially expressed genes (DEGs) and using the genes identified
670 in the STEM analysis, separately. Gee-set over-representation analysis (ORA) of GO
671 Biological Process (GOBP), GO Molecular Function (GOMF), and GO Cellular Compartment
672 (GOCC) terms were performed using the enrichGO function of clusterProfiler package
673 version 3.18.0. Minimum and maximum gene set sizes were set to 10 and 500, respectively.
674 Results were simplified using the simplify function of clusterProfiler with the similarity cut-
675 off set to 0.7 and minimum adjusted p-value used as the feature for selecting the
676 representative terms. Enrichment results with adjusted p-values below 0.05 and at least 3
677 core enrichment genes were considered significantly enriched. ORA of KEGG and
678 REACTOME pathway terms were performed using the enrichKEGG and enrichPathway
679 functions of clusterProfiler. Minimum and maximum gene set sizes were set to 10 and 500,
680 respectively. The same significance criteria for the enrichments were used as for the GO
681 term enrichments. Results of the enrichment results were visualised as barplots or as pie

682 charts. Barplots were made using the `ggbarplot` function of R package (R studio version
683 2021.09.2), `ggpubr` version 0.4.0, showing a maximum of five pathways with adjusted p-
684 value below 0.05 *per* pathway category. Pie charts were made using Prism GraphPad version
685 9.0.

686 **5.4.5 Protein-protein interaction network analysis**

687 The search tool for retrieval of interacting genes (STRING) (<https://string-db.org>)
688 database, which integrates both known and predicted PPIs, was used to predict functional
689 interactions of proteins (Szkarczyk et al., 2021). Active interaction sources, including text
690 mining, experiments, databases, and co-expression as well as species limited to “*Danio*
691 *rerio*” and an interaction score > 0.7 (high confidence) were applied to construct the PPI
692 networks. The network was further clustered using *k-means* clustering to a specific number
693 of up to 3 clusters.

694

695 **5.4.6 Venn Diagram analysis**

696 Venn Diagram analysis was performed using the online tool Venny 2.1.0 – BioinfoGP
697 (<https://bioinfo.gp.cnb.csic.es/tools/venny/>) (Oliveros, 2007-2015).

698

699 **5.4.7 Statistical analysis**

700 A chi-square test was used in **Fig 5** to compare between the relative chromosome
701 location of telomerase-dependent genes in the gut and brain, using raw data values, even
702 though it is the % that is represented in the graphs, to ensure accurate analysis. P value
703 <0.05 was considered significant and denoted with a *, whereas ns was used to denote non-
704 significant differences.

705

706 **ACKNOWLEDGEMENTS**

707 The authors would like to acknowledge Genevia Technologies Oy for the main bulk of
708 RNA sequencing analysis service. We are very grateful to Joao Ribeiro for valuable advice
709 regarding the many functionalities of Microsoft Excel, which greatly facilitated data analysis.
710 This work was generously funded by a University of Sheffield PhD studentship to RRM, a

711 Sheffield University Vice Chancellor's Research Fellowship and a Wellcome Trust/Royal
712 Society Sir Henry Dale Fellowship (UNS35121) to CMH.

713

714 **AUTHOR CONTRIBUTIONS**

715 RRM and CMH conceived and designed this work; RRM performed additional RNA
716 sequencing beyond that provided by Genevia services; RRM, MR and CMH analysed and
717 interpreted RNA sequencing results and co-wrote the manuscript; CMH designed the figures
718 with input from co-authors.

719

720 **COMPETING INTERESTS**

721 The authors declare no competing interests

722

723

724 **DATA AVAILABILITY STATEMENT**

725 The RNA sequencing data from this experiment were deposited in gene expression
726 omnibus (GEO) and will be made available when in peer review.

727

728 **ORCID**

729 Raquel Rua Martins: <https://orcid.org/0000-0003-3952-8649>

730 Michael Rera: <https://orcid.org/0000-0002-6574-6511>

731 Catarina Martins Henriques: <https://orcid.org/0000-0003-1882-756X>

732

733 **SUPPORTING INFORMATION**

734 Supporting information in the form of figures, tables and source data can be found
735 online in the Supportive information section at the end of the article

736

737 **REFERENCES**

738

- 739 Ahmed, S., Passos, J. F., Birket, M. J., Beckmann, T., Brings, S., Peters, H., . . . Saretzki, G.
740 (2008). Telomerase does not counteract telomere shortening but protects
741 mitochondrial function under oxidative stress. *J Cell Sci*, *121*(Pt 7), 1046-1053.
742 doi:10.1242/jcs.019372
- 743 Anchelin, M., Alcaraz-Perez, F., Martinez, C. M., Bernabe-Garcia, M., Mulero, V., & Cayuela,
744 M. L. (2013). Premature aging in telomerase-deficient zebrafish. *Dis Model Mech*,
745 *6*(5), 1101-1112. doi:10.1242/dmm.011635
- 746 Baker, D. J., Childs, B. G., Durik, M., Wijers, M. E., Sieben, C. J., Zhong, J., . . . van Deursen, J.
747 M. (2016). Naturally occurring p16(Ink4a)-positive cells shorten healthy lifespan.
748 *Nature*, *530*(7589), 184-189. doi:10.1038/nature16932
- 749 Baker, D. J., Wijshake, T., Tchkonja, T., LeBrasseur, N. K., Childs, B. G., van de Sluis, B., . . .
750 van Deursen, J. M. (2011). Clearance of p16Ink4a-positive senescent cells delays
751 ageing-associated disorders. *Nature*, *479*(7372), 232-236. doi:10.1038/nature10600
- 752 Basak, O., van de Born, M., Korving, J., Beumer, J., van der Elst, S., van Es, J. H., & Clevers, H.
753 (2014). Mapping early fate determination in Lgr5+ crypt stem cells using a novel
754 Ki67-RFP allele. *EMBO J*, *33*(18), 2057-2068. doi:10.15252/embj.201488017
- 755 Bertaglia, E., Jensen, K. K., Castro-Perez, J., Xu, Y., Di Paolo, G., Chan, R. B., . . . Haeusler, R.
756 A. (2017). Cyp8b1 ablation prevents Western diet-induced weight gain and hepatic
757 steatosis because of impaired fat absorption. *Am J Physiol Endocrinol Metab*, *313*(2),
758 E121-E133. doi:10.1152/ajpendo.00409.2016
- 759 Blackburn, E. H., Epel, E. S., & Lin, J. (2015). Human telomere biology: A contributory and
760 interactive factor in aging, disease risks, and protection. *Science*, *350*, 1193-1198.
761 doi:10.1126/science.aab3389
- 762 Bodnar, A. G. (1998). Extension of Life-Span by Introduction of Telomerase into Normal
763 Human Cells. *Science*, *279*(5349), 349-352. doi:10.1126/science.279.5349.349
- 764 Boutouja, F., Stiehm, C. M., & Platta, H. W. (2019). mTOR: A Cellular Regulator Interface in
765 Health and Disease. *Cells*, *8*(1). doi:10.3390/cells8010018
- 766 Cao, Y., Li, H., Deb, S., & Liu, J. P. (2002). TERT regulates cell survival independent of
767 telomerase enzymatic activity. *Oncogene*, *21*(20), 3130-3138.
768 doi:10.1038/sj.onc.1205419
- 769 Cardoso, B. a., Gírio, a., Henriques, C., Martins, L. R., Santos, C., Silva, a., & Barata, J. T.
770 (2008). Aberrant signaling in T-cell acute lymphoblastic leukemia: Biological and
771 therapeutic implications. *Brazilian Journal of Medical and Biological Research*, *41*,
772 344-350. doi:10.1590/S0100-879X2008005000016
- 773 Carneiro, M. C., de Castro, I. P., & Ferreira, M. G. (2016). Telomeres in aging and disease:
774 lessons from zebrafish. *Dis Model Mech*, *9*(7), 737-748. doi:10.1242/dmm.025130
- 775 Carneiro, M. C., Henriques, C. M., Nabais, J., Ferreira, T., Carvalho, T., & Ferreira, M. G.
776 (2016). Short Telomeres in Key Tissues Initiate Local and Systemic Aging in Zebrafish.
777 *PLoS Genet*, *12*, e1005798. doi:10.1371/journal.pgen.1005798
- 778 Choi, J., Southworth, L. K., Sarin, K. Y., Venteicher, A. S., Ma, W., Chang, W., . . . Artandi, S. E.
779 (2008). TERT promotes epithelial proliferation through transcriptional control of a
780 Myc- and Wnt-related developmental program. *PLoS Genet*, *4*(1), e10.
781 doi:10.1371/journal.pgen.0040010
- 782 d'Adda di Fagagna, F., Reaper, P. M., Clay-Farrace, L., Fiegler, H., Carr, P., Von Zglinicki, T., . .
783 . Jackson, S. P. (2003). A DNA damage checkpoint response in telomere-initiated
784 senescence. *Nature*, *426*(6963), 194-198. doi:10.1038/nature02118

- 785 Dambrose, E., Monnier, L., Ruisheng, L., Aguilaniu, H., Joly, J. S., Tricoire, H., & Rera, M.
786 (2016). Two phases of aging separated by the Smurf transition as a public path to
787 death. *Sci Rep*, 6, 23523. doi:10.1038/srep23523
- 788 De Felice, B., Annunziata, A., Fiorentino, G., Manfredotto, F., D'Alessandro, R., Marino, R., . . .
789 Biffali, E. (2014). Telomerase expression in amyotrophic lateral sclerosis (ALS)
790 patients. *J Hum Genet*, 59(10), 555-561. doi:10.1038/jhg.2014.72
- 791 de Jong, P. R., Gonzalez-Navajas, J. M., & Jansen, N. J. (2016). The digestive tract as the
792 origin of systemic inflammation. *Crit Care*, 20(1), 279. doi:10.1186/s13054-016-1458-
793 3
- 794 de Lange, T. (2004). T-loops and the origin of telomeres. *Nature reviews. Molecular cell*
795 *biology*, 5, 323-329. doi:10.1038/nrm1422
- 796 Deacon, K., & Knox, A. J. (2018). PINX1 and TERT Are Required for TNF-alpha-Induced Airway
797 Smooth Muscle Chemokine Gene Expression. *J Immunol*, 200(4), 1283-1294.
798 doi:10.4049/jimmunol.1700414
- 799 Dimri, G. P., Lee, X., Basile, G., Acosta, M., Scott, G., Roskelley, C., . . . et al. (1995). A
800 biomarker that identifies senescent human cells in culture and in aging skin in vivo.
801 *Proc Natl Acad Sci U S A*, 92(20), 9363-9367.
- 802 Eitan, E., Tichon, A., Gazit, A., Gitler, D., Slavin, S., & Priel, E. (2012). Novel telomerase-
803 increasing compound in mouse brain delays the onset of amyotrophic lateral
804 sclerosis. *EMBO Mol Med*, 4(4), 313-329. doi:10.1002/emmm.201200212
- 805 England, P. H. (2017). *Chapter 1: life expectancy and healthy life expectancy*. Retrieved from
806 [https://www.gov.uk/government/publications/health-profile-for-england/chapter-1-](https://www.gov.uk/government/publications/health-profile-for-england/chapter-1-life-expectancy-and-healthy-life-expectancy#references)
807 [life-expectancy-and-healthy-life-expectancy#references](https://www.gov.uk/government/publications/health-profile-for-england/chapter-1-life-expectancy-and-healthy-life-expectancy#references).
- 808 Ernst, J., & Bar-Joseph, Z. (2006). STEM: a tool for the analysis of short time series gene
809 expression data. *BMC Bioinformatics*, 7, 191. doi:10.1186/1471-2105-7-191
- 810 Ferreira, M. G., Miller, K. M., & Cooper, J. P. (2004). Indecent exposure: when telomeres
811 become uncapped. *Mol Cell*, 13(1), 7-18.
- 812 Forsyth, N. R., Wright, W. E., & Shay, J. W. (2002). Telomerase and differentiation in
813 multicellular organisms: turn it off, turn it on, and turn it off again. *Differentiation*,
814 69(4-5), 188-197. doi:10.1046/j.1432-0436.2002.690412.x
- 815 Gerhardt, T., & Ley, K. (2015). Monocyte trafficking across the vessel wall. *Cardiovascular*
816 *Research*, 107(3), 321-330. doi:10.1093/cvr/cvv147
- 817 Ghosh, A., Saginc, G., Leow, S. C., Khattar, E., Shin, E. M., Yan, T. D., . . . Tergaonkar, V.
818 (2012). Telomerase directly regulates NF-kappaB-dependent transcription. *Nat Cell*
819 *Biol*, 14(12), 1270-1281. doi:10.1038/ncb2621
- 820 Gladyshev, V. N. (2021). The Ground Zero of Organismal Life and Aging. *Trends Mol Med*,
821 27(1), 11-19. doi:10.1016/j.molmed.2020.08.012
- 822 Gomes, N. M. V., Ryder, O. a., Houck, M. L., Charter, S. J., Walker, W., Forsyth, N. R., . . .
823 Wright, W. E. (2011). Comparative biology of mammalian telomeres: hypotheses on
824 ancestral states and the roles of telomeres in longevity determination. *Aging Cell*,
825 10, 761-768. doi:10.1111/j.1474-9726.2011.00718.x
- 826 Goodman, W. A., & Jain, M. K. (2011). Length does not matter: A new take on telomerase
827 reverse transcriptase. *Arteriosclerosis, thrombosis, and vascular biology*, 31, 235-
828 236. doi:10.1161/ATVBAHA.110.220343
- 829 Greider, C. W., & Blackburn, E. H. (1985). Identification of a specific telomere terminal
830 transferase activity in Tetrahymena extracts. *Cell*, 43(2 Pt 1), 405-413.
831 doi:10.1016/0092-8674(85)90170-9

- 832 Haendeler, J., Drose, S., Buchner, N., Jakob, S., Altschmied, J., Goy, C., . . . Dimmeler, S.
833 (2009). Mitochondrial telomerase reverse transcriptase binds to and protects
834 mitochondrial DNA and function from damage. *Arterioscler Thromb Vasc Biol*, *29*(6),
835 929-935. doi:10.1161/ATVBAHA.109.185546
- 836 Hagey, D. W., Topcic, D., Kee, N., Reynaud, F., Bergsland, M., Perlmann, T., & Muhr, J.
837 (2020). CYCLIN-B1/2 and -D1 act in opposition to coordinate cortical progenitor self-
838 renewal and lineage commitment. *Nat Commun*, *11*(1), 2898. doi:10.1038/s41467-
839 020-16597-8
- 840 Hayflick, L. (2007). Biological aging is no longer an unsolved problem. *Ann N Y Acad Sci*,
841 *1100*, 1-13. doi:10.1196/annals.1395.001
- 842 Henriques, C. M., Carneiro, M. C., Tenente, I. M., Jacinto, A., & Ferreira, M. G. (2013).
843 Telomerase is required for zebrafish lifespan. *PLoS Genet*, *9*(1), e1003214.
844 doi:10.1371/journal.pgen.1003214
- 845 Henriques, C. M., & Ferreira, M. G. (2012). Consequences of telomere shortening during
846 lifespan. *Curr Opin Cell Biol*, *24*(6), 804-808. doi:10.1016/j.ceb.2012.09.007
- 847 Hong, S. N., Joung, J. G., Bae, J. S., Lee, C. S., Koo, J. S., Park, S. J., . . . Kim, Y. H. (2017). RNA-
848 seq Reveals Transcriptomic Differences in Inflamed and Noninflamed Intestinal
849 Mucosa of Crohn's Disease Patients Compared with Normal Mucosa of Healthy
850 Controls. *Inflamm Bowel Dis*, *23*(7), 1098-1108.
851 doi:10.1097/MIB.0000000000001066
- 852 Ifergan, I., Kébir, H., Bernard, M., Wosik, K., Dodelet-Devillers, A., Cayrol, R., . . . Prat, A.
853 (2007). The blood–brain barrier induces differentiation of migrating monocytes into
854 Th17-polarizing dendritic cells. *Brain*, *131*(3), 785-799. doi:10.1093/brain/awm295
- 855 Jaskelioff, M., Muller, F. L., Paik, J.-H., Thomas, E., Jiang, S., Adams, A. C., . . . Depinho, R. a.
856 (2011). Telomerase reactivation reverses tissue degeneration in aged telomerase-
857 deficient mice. *Nature*, *469*, 102-106. doi:10.1038/nature09603
- 858 Jurk, D., Wang, C., Miwa, S., Maddick, M., Korolchuk, V., Tzolou, A., . . . von Zglinicki, T.
859 (2012). Postmitotic neurons develop a p21-dependent senescence-like phenotype
860 driven by a DNA damage response. *Aging Cell*, *11*(6), 996-1004. doi:10.1111/j.1474-
861 9726.2012.00870.x
- 862 Lange, C., Rost, F., Machate, A., Reinhardt, S., Lesche, M., Weber, A., . . . Brand, M. (2020).
863 Single cell sequencing of radial glia progeny reveals the diversity of newborn neurons
864 in the adult zebrafish brain. *Development*, *147*(1). doi:10.1242/dev.185595
- 865 Lawson, N. D., Li, R., Shin, M., Grosse, A., Yukselen, O., Stone, O. A., . . . Zhu, L. (2020). An
866 improved zebrafish transcriptome annotation for sensitive and comprehensive
867 detection of cell type-specific genes. *Elife*, *9*. doi:10.7554/eLife.55792
- 868 Lee, H. W., Blasco, M. A., Gottlieb, G. J., Horner, J. W., 2nd, Greider, C. W., & DePino, R. A.
869 (1998). Essential role of mouse telomerase in highly proliferative organs. *Nature*,
870 *392*(6676), 569-574. doi:10.1038/33345
- 871 Lee, J., Jo, Y. S., Sung, Y. H., Hwang, I. K., Kim, H., Kim, S. Y., . . . Lee, H. W. (2010).
872 Telomerase deficiency affects normal brain functions in mice. *Neurochem Res*, *35*(2),
873 211-218. doi:10.1007/s11064-009-0044-3
- 874 Lemoine, M. (2021). The Evolution of the Hallmarks of Aging. *Front Genet*, *12*, 693071.
875 doi:10.3389/fgene.2021.693071
- 876 Lentini, L., Barra, V., Schillaci, T., & Di Leonardo, A. (2012). MAD2 depletion triggers
877 premature cellular senescence in human primary fibroblasts by activating a p53

- 878 pathway preventing aneuploid cells propagation. *J Cell Physiol*, 227(9), 3324-3332.
879 doi:10.1002/jcp.24030
- 880 Li, L., Song, J., Chuquisana, O., Hannocks, M. J., Loismann, S., Vogl, T., . . . Sorokin, L. (2020).
881 Endothelial Basement Membrane Laminins as an Environmental Cue in Monocyte
882 Differentiation to Macrophages. *Front Immunol*, 11, 584229.
883 doi:10.3389/fimmu.2020.584229
- 884 The hallmarks of aging, 153 (2013).
- 885 Lu, Z., Ding, L., Lu, Q., & Chen, Y. H. (2013). Claudins in intestines: Distribution and functional
886 significance in health and diseases. *Tissue Barriers*, 1(3), e24978.
887 doi:10.4161/tisb.24978
- 888 Mattiussi, M., Tilman, G., Lenglez, S., & Decottignies, A. (2012). Human telomerase
889 represses ROS-dependent cellular responses to Tumor Necrosis Factor- α without
890 affecting NF- κ B activation. *Cellular signalling*, 24, 708-717.
891 doi:10.1016/j.cellsig.2011.11.004
- 892 Morris, M., Hepburn, P., & Wynford-Thomas, D. (2002). Sequential extension of proliferative
893 lifespan in human fibroblasts induced by over-expression of CDK4 or 6 and loss of
894 p53 function. *Oncogene*, 21(27), 4277-4288. doi:10.1038/sj.onc.1205492
- 895 Neale, B. M., Fagerness, J., Reynolds, R., Sobrin, L., Parker, M., Raychaudhuri, S., . . . Seddon,
896 J. M. (2010). Genome-wide association study of advanced age-related macular
897 degeneration identifies a role of the hepatic lipase gene (LIPC). *Proc Natl Acad Sci U S*
898 *A*, 107(16), 7395-7400. doi:10.1073/pnas.0912019107
- 899 Nersisyan, L., Hopp, L., Loeffler-Wirth, H., Galle, J., Loeffler, M., Arakelyan, A., & Binder, H.
900 (2019). Telomere Length Maintenance and Its Transcriptional Regulation in Lynch
901 Syndrome and Sporadic Colorectal Carcinoma. *Front Oncol*, 9, 1172.
902 doi:10.3389/fonc.2019.01172
- 903 Oliveros, J. C. (2007-2015). Venny. An interactive tool for comparing lists with Venn's
904 diagrams. Retrieved from <https://bioinfogp.cnb.csic.es/tools/venny/index.html>
- 905 Ovadya, Y., & Krizhanovsky, V. (2014). Senescent cells: SASPected drivers of age-related
906 pathologies. *Biogerontology*, 15, 627-642. doi:10.1007/s10522-014-9529-9
- 907 Pam S. Ellis, R. R. M., Emily J. Thompson, Asma Farhat, Stephen A. Renshaw, Catarina M.
908 Henriques. (2022). *A subset of gut leukocytes have telomerase-dependent "hyper-*
909 *long" telomeres and require telomerase for function in zebrafish*. Biorxiv.
- 910 Pekalski, M. L., Ferreira, R. C., Coulson, R. M., Cutler, A. J., Guo, H., Smyth, D. J., . . . Wicker,
911 L. S. (2013). Postthymic expansion in human CD4 naive T cells defined by expression
912 of functional high-affinity IL-2 receptors. *J Immunol*, 190(6), 2554-2566.
913 doi:10.4049/jimmunol.1202914
- 914 Poehlmann, A., Habold, C., Walluscheck, D., Reissig, K., Bajbouj, K., Ullrich, O., . . . Schneider-
915 Stock, R. (2011). Cutting edge: Chk1 directs senescence and mitotic catastrophe in
916 recovery from G(2) checkpoint arrest. *J Cell Mol Med*, 15(7), 1528-1541.
917 doi:10.1111/j.1582-4934.2010.01143.x
- 918 Pruitt, S. C., Bailey, K. J., & Freeland, A. (2007). Reduced Mcm2 expression results in severe
919 stem/progenitor cell deficiency and cancer. *Stem Cells*, 25(12), 3121-3132.
920 doi:10.1634/stemcells.2007-0483
- 921 Rahman, R., Latonen, L., & Wiman, K. G. (2005). hTERT antagonizes p53-induced apoptosis
922 independently of telomerase activity. *Oncogene*, 24(8), 1320-1327.
923 doi:10.1038/sj.onc.1208232

- 924 Raj, D. D. A., Moser, J., van der Pol, S. M. A., van Os, R. P., Holtman, I. R., Brouwer, N., . . .
925 Boddeke, H. W. G. M. (2015). Enhanced microglial pro-inflammatory response to
926 lipopolysaccharide correlates with brain infiltration and blood-brain barrier
927 dysregulation in a mouse model of telomere shortening. *Aging Cell*, 1003-1013.
928 doi:10.1111/accel.12370
- 929 Rando, T. A., & Wyss-Coray, T. (2021). Asynchronous, contagious and digital aging. *Nat*
930 *Aging*, 1(1), 29-35. doi:10.1038/s43587-020-00015-1
- 931 Rera, M., Azizi, M. J., & Walker, D. W. (2013). Organ-specific mediation of lifespan extension:
932 more than a gut feeling? *Ageing Res Rev*, 12(1), 436-444.
933 doi:10.1016/j.arr.2012.05.003
- 934 Rera, M., Clark, R. I., & Walker, D. W. (2012). Intestinal barrier dysfunction links metabolic
935 and inflammatory markers of aging to death in *Drosophila*. *Proc Natl Acad Sci U S A*,
936 109(52), 21528-21533. doi:10.1073/pnas.1215849110
- 937 Ripa, R., Dolfi, L., Terrigno, M., Pandolfini, L., Savino, A., Arcucci, V., . . . Cellierino, A. (2017).
938 MicroRNA miR-29 controls a compensatory response to limit neuronal iron
939 accumulation during adult life and aging. *BMC Biol*, 15(1), 9. doi:10.1186/s12915-
940 017-0354-x
- 941 Robin, J. D., Ludlow, A. T., Batten, K., Magdinier, F., Stadler, G., Wagner, K. R., . . . Wright, W.
942 E. (2014). Telomere position effect: regulation of gene expression with progressive
943 telomere shortening over long distances. *Genes Dev*, 28(22), 2464-2476.
944 doi:10.1101/gad.251041.114
- 945 Romaniuk, A., Paszel-Jaworska, A., Toton, E., Lisiak, N., Holysz, H., Krolak, A., . . . Rubis, B.
946 (2018). The non-canonical functions of telomerase: to turn off or not to turn off. *Mol*
947 *Biol Rep*. doi:10.1007/s11033-018-4496-x
- 948 Rudnicka, E., Napierala, P., Podfigurna, A., Meczekalski, B., Smolarczyk, R., & Grymowicz, M.
949 (2020). The World Health Organization (WHO) approach to healthy ageing.
950 *Maturitas*, 139, 6-11. doi:10.1016/j.maturitas.2020.05.018
- 951 Santamarina-Fojo, S., Gonzalez-Navarro, H., Freeman, L., Wagner, E., & Nong, Z. (2004).
952 Hepatic lipase, lipoprotein metabolism, and atherogenesis. *Arterioscler Thromb Vasc*
953 *Biol*, 24(10), 1750-1754. doi:10.1161/01.ATV.0000140818.00570.2d
- 954 Sarin, K. Y., Cheung, P., Gilison, D., Lee, E., Tennen, R. I., Wang, E., . . . Artandi, S. E. (2005).
955 Conditional telomerase induction causes proliferation of hair follicle stem cells.
956 *Nature*, 436(7053), 1048-1052. doi:10.1038/nature03836
- 957 Schaum, N., Lehallier, B., Hahn, O., Palovics, R., Hosseinzadeh, S., Lee, S. E., . . . Wyss-Coray,
958 T. (2020). Ageing hallmarks exhibit organ-specific temporal signatures. *Nature*,
959 583(7817), 596-602. doi:10.1038/s41586-020-2499-y
- 960 Scheinin, T., Bohling, T., Halme, L., Kontiainen, S., Bjorge, L., & Meri, S. (1999). Decreased
961 expression of protectin (CD59) in gut epithelium in ulcerative colitis and Crohn's
962 disease. *Hum Pathol*, 30(12), 1427-1430. doi:10.1016/s0046-8177(99)90163-6
- 963 Schenkel, A. R., Mamdouh, Z., Chen, X., Liebman, R. M., & Muller, W. A. (2002). CD99 plays a
964 major role in the migration of monocytes through endothelial junctions. *Nature*
965 *immunology*, 3(2), 143-150. doi:10.1038/ni749
- 966 Schmidt, S., Schneider, L., Essmann, F., Cirstea, I. C., Kuck, F., Kletke, A., . . . Piekorz, R. P.
967 (2010). The centrosomal protein TACC3 controls paclitaxel sensitivity by modulating
968 a premature senescence program. *Oncogene*, 29(46), 6184-6192.
969 doi:10.1038/onc.2010.354

- 970 Segal-Bendirdjian, E., & Geli, V. (2019). Non-canonical Roles of Telomerase: Unraveling the
971 Imbroglia. *Front Cell Dev Biol*, 7, 332. doi:10.3389/fcell.2019.00332
- 972 Shokhirev, M. N., & Johnson, A. A. (2021). Modeling the human aging transcriptome across
973 tissues, health status, and sex. *Aging Cell*, 20(1), e13280. doi:10.1111/accel.13280
- 974 Smith, L. K., He, Y., Park, J. S., Bieri, G., Snethlage, C. E., Lin, K., . . . Villeda, S. A. (2015).
975 beta2-microglobulin is a systemic pro-aging factor that impairs cognitive function
976 and neurogenesis. *Nat Med*, 21(8), 932-937. doi:10.1038/nm.3898
- 977 Spilsbury, A., Miwa, S., Attems, J., & Saretzki, G. (2015). The role of telomerase protein TERT
978 in Alzheimer's disease and in tau-related pathology in vitro. *J Neurosci*, 35(4), 1659-
979 1674. doi:10.1523/JNEUROSCI.2925-14.2015
- 980 Sullivan, D. I., Jiang, M., Hinchie, A. M., Roth, M. G., Bahudhanapati, H., Nouraie, M., . . .
981 Alder, J. K. (2021). Transcriptional and Proteomic Characterization of Telomere-
982 Induced Senescence in a Human Alveolar Epithelial Cell Line. *Front Med (Lausanne)*,
983 8, 600626. doi:10.3389/fmed.2021.600626
- 984 Sung, Y. H., Ali, M., & Lee, H. W. (2014). Extracting extra-telomeric phenotypes from
985 telomerase mouse models. *Yonsei Medical Journal*, 55, 1-8.
986 doi:10.3349/ymj.2014.55.1.1
- 987 Szklarczyk, D., Gable, A. L., Nastou, K. C., Lyon, D., Kirsch, R., Pyysalo, S., . . . von Mering, C.
988 (2021). The STRING database in 2021: customizable protein-protein networks, and
989 functional characterization of user-uploaded gene/measurement sets. *Nucleic Acids*
990 *Res*, 49(D1), D605-D612. doi:10.1093/nar/gkaa1074
- 991 Tabula Muris, C. (2020). A single-cell transcriptomic atlas characterizes ageing tissues in the
992 mouse. *Nature*, 583(7817), 590-595. doi:10.1038/s41586-020-2496-1
- 993 Tacutu, R., Thornton, D., Johnson, E., Budovsky, A., Barardo, D., Craig, T., . . . de Magalhaes,
994 J. P. (2018). Human Ageing Genomic Resources: new and updated databases. *Nucleic*
995 *Acids Res*, 46(D1), D1083-D1090. doi:10.1093/nar/gkx1042
- 996 Tricoire, H., & Rera, M. (2015). A New, Discontinuous 2 Phases of Aging Model: Lessons from
997 *Drosophila melanogaster*. *PLoS One*, 10(11), e0141920.
998 doi:10.1371/journal.pone.0141920
- 999 Ugalde, A. P., Ramsay, A. J., de la Rosa, J., Varela, I., Marino, G., Cadinanos, J., . . . Lopez-
1000 Otin, C. (2011). Aging and chronic DNA damage response activate a regulatory
1001 pathway involving miR-29 and p53. *EMBO J*, 30(11), 2219-2232.
1002 doi:10.1038/emboj.2011.124
- 1003 Watt, P. M., & Hickson, I. D. (1994). Structure and function of type II DNA topoisomerases.
1004 *Biochem J*, 303 (Pt 3), 681-695. doi:10.1042/bj3030681
- 1005 Wienholds, E., van Eeden, F., Kosters, M., Mudde, J., Plasterk, R. H., & Cuppen, E. (2003).
1006 Efficient target-selected mutagenesis in zebrafish. *Genome Res*, 13(12), 2700-2707.
1007 doi:10.1101/gr.1725103
- 1008 Zhang, H., Weyand, C. M., & Goronzy, J. J. (2021). Hallmarks of the aging T-cell system. *FEBS*
1009 *J*, 288(24), 7123-7142. doi:10.1111/febs.15770
- 1010 Zhang, M. J., Pisco, A. O., Darmanis, S., & Zou, J. (2021). Mouse aging cell atlas analysis
1011 reveals global and cell type-specific aging signatures. *Elife*, 10.
1012 doi:10.7554/eLife.62293
- 1013 Zhao, Y., Hasse, S., & Bourgoin, S. G. (2021). Phosphatidylserine-specific phospholipase A1: A
1014 friend or the devil in disguise. *Prog Lipid Res*, 83, 101112.
1015 doi:10.1016/j.plipres.2021.101112

1016 Zhu, S., Paydar, M., Wang, F., Li, Y., Wang, L., Barrette, B., . . . Peng, A. (2020). Kinesin Kif2C
1017 in regulation of DNA double strand break dynamics and repair. *Elife*, 9.
1018 doi:10.7554/eLife.53402
1019

1020

1021 **FIGURE LEGENDS**

1022

1023 **Graphical Abstract:** Although the gut and brain have distinct transcriptomic signatures of
1024 ageing, both tissues display hallmarks of ageing as early as 9 months in the WT zebrafish.
1025 Importantly, telomerase depletion accelerates the appearance of such hallmarks in both gut
1026 and brain. In specific, the *tert*^{-/-} gut at 2 months and the *tert*^{-/-} brain at 9 months display
1027 similar distribution of the mainly affected hallmarks of ageing, in the WT old gut and brain at
1028 35 months of age. We identified stem cell exhaustion (light red) as the common principal
1029 hallmark of ageing at the early stages of ageing, in both tissues. Finally, we further identified
1030 altered intercellular communication (light green), in which immunity and inflammation play
1031 a central role, as the main telomerase-dependent hallmark of ageing common between the
1032 gut and brain.

1033 **Fig 1. Summary of the experimental design and principal component analysis (PCA).** (A)
1034 RNA-Sequencing was performed in whole gut and brain tissues from WT and *tert*^{-/-}
1035 zebrafish, at different timepoints throughout their lifespan. Age-associated transcriptomic
1036 changes were analysed using two different methods: time-series analysis (genes that change
1037 consistently overtime) and all differentially expressed genes (ALL DEGs; genes whose
1038 expression is altered over-time, in both genotypes, as compared with the WT young
1039 baseline. (B) PCA representing the variation in the data from gut (gold) and brain (pink)
1040 tissues, in both WT and *tert*^{-/-} fish. (C-D) PCA showing the variation in the data from fish at
1041 different ages (2 months, pink; 9 months, green; 22 months, blue; 35 months, purple), in WT
1042 (circle) versus *tert*^{-/-} fish (triangle), in (C) gut and (D) brain samples. PCA was performed
1043 using the plotPCA function of DESeq2 and considering the top 500 genes with highest
1044 variance across the samples. (E) Summary of the number of significantly de-regulated genes
1045 at each time-point, in both genotypes, in gut (E1) and brain (E2) tissues, over-time, as
1046 compared with the WT young baseline.

1047

1048 **Fig 2. Identification of time-dependent signatures of ageing in the WT and *tert*^{-/-} zebrafish**
1049 **gut and brain.** (A, B) Transcriptomic temporal profiles in the (A) gut and brain (B) of WT
1050 (black) and *tert*^{-/-} fish (red) were identified using the Short Time-series Expression Miner
1051 (STEM) and are represented in line plots. The thicker lines on the plots represent the
1052 median fold change of each profile. For each temporal profile, enrichment analysis was
1053 performed using the enrichGO, enrichKEGG, and enrichPathway functions of clusterProfiler
1054 package version 3.18.0. Processes and pathways from each temporal profile were further
1055 classified and grouped according to the main hallmarks of ageing (Lemoine, 2021; López-
1056 Otín et al., 2013), which is represented in pie charts. (A1, B1) A summary of the enrichment
1057 analysis of one of the profiles is represented in the bar plots, where processes and pathways
1058 are represented in different colours according to the classification into hallmarks of ageing.
1059 This summary contains the top enriched processes and pathways from each database (p-
1060 value >0.05 and at least 3 core enrichment genes; up to 5 terms *per* database: GOBP, GOCC,
1061 GOMF, KEEG, and REACTOME).

1062

1063 **Fig 3. Qualitative changes in the hallmarks of ageing over-time, comparing WT and *tert*^{-/-}**
1064 **zebrafish gut and brain.** The age-associated enriched processes and pathways identified in
1065 the previous figures were further re-classified and grouped into the main well-known
1066 hallmarks of ageing. (A-B) Pie charts represent the hallmarks of ageing identified in the (A)
1067 gut and (B) brain, at different ages throughout WT (black) and *tert*^{-/-} (red) zebrafish lifespan.
1068 This analysis was performed considering the (A1, B1) genes identified in the temporal
1069 profiles (within STEM), (A2, B2) all the genes differentially expressed at any timepoint
1070 (within ALL DEGs), and (A3, B3) STEM and ALL DEGs combined. (A4, B4) The number of
1071 transcriptomic changes increases with ageing in both (A4) gut and (B4) brain, independently
1072 of the phenotype, when considering either the genes within STEM or the genes within ALL
1073 DEGs.

1074

1075 **Fig 4. Determining at which age *tert*^{-/-} share more genes associated with the hallmarks of**
1076 **ageing, with the naturally aged WT.** (A) Venn diagrams highlight the number of genes
1077 associated with hallmarks of ageing in common between old WT (35 months) and *tert*^{-/-} at
1078 the different ages tested, in (A.1) gut and (A.2) brain tissues. Data show that the *tert*^{-/-} gut at
1079 2 months has the most number genes associated with hallmarks of ageing in common with

1080 old WT gut. The *tert*^{-/-} brain at 22 months has the most number genes associated with
1081 hallmarks of ageing in common with old WT brain. The respective lists of genes shared
1082 between old WT gut and *tert*^{-/-} gut at 2 months and old WT brain and *tert*^{-/-} 22-month brain
1083 are shown in B (B.1 gut, B.2, brain). (B1.1, B1.2) Gene networks with the genes identified in
1084 B.1 and B.2 were performed (B1.1 and B1.2, respectively) by K-means clustering using String
1085 software. These include the genes identified in the temporal profiles (from STEM) and in
1086 ALL DEGs.

1087

1088 **Fig 5. Identifying *tert*-dependent gene changes in zebrafish gut and brain ageing and their**
1089 **chromosome location in relation to the telomeric end.** (A-B) Gene alterations that are
1090 anticipated in the *tert*^{-/-} when comparing with WT at the same age (i.e., telomerase-
1091 dependent). (A1, B1) Protein-protein interaction network of these genes highlights clusters
1092 of genes associated with (A1) metabolic processes in the gut and clusters of genes
1093 associated with (B1) cell cycle, genome instability and immune system in the brain. (C) Genes
1094 located at the end of the chromosome (i.e., <10MB from chromosome end) are likely to be
1095 directly affected by telomere shortening due to the telomere positioning effect (TPE). The
1096 data show that there is no significant difference between telomerase-dependent and -
1097 independent genes, in what concerns their proximity to the chromosome end, in either gut
1098 (C2) or brain (C3). However, there is a significantly higher number of telomerase-dependent
1099 genes located at the end of chromosomes in the gut than in the brain (C4).

1100

1101 **Fig 6. Determining genes and pathways altered with ageing that are in common between**
1102 **gut and brain.** (A) Graph represents WT zebrafish lifespan and highlights 'early' and 'late'
1103 stages of ageing. (A.1) All genes identified in common between gut and brain at early (9
1104 months) and late (35 months) stages of ageing. *G and *B represent telomerase-dependent
1105 genes in the Gut or in the Brain, respectively. (B-C) Protein-protein interaction networks
1106 with the genes found in common between the gut and brain at (B) early and (C) late stages
1107 of ageing were performed using STRING software. These include the genes identified in the
1108 temporal profiles (from STEM) and in ALL DEGs.

1109

1110

1111

1112 **SUPPLEMENTARY FIGURE LEGENDS**

1113 **Supplementary Fig 1. Genes associated with the hallmarks of ageing that are in common**
1114 **between 35-months-old WT and *tert*^{-/-} at different ages, in the (A1) gut and (A2) brain.** The
1115 different colours represent different hallmarks of ageing: purple, loss of proteostasis;
1116 yellow, mitochondrial dysfunction; green, altered intercellular communication. These
1117 include the genes identified in the temporal profiles (from STEM) and in ALL DEGs.

1118

1119 **Supplementary Fig 2. Protein-protein interaction network and cluster analysis of gene**
1120 **changes in WT at the ‘origins’ versus ‘later’ stages of ageing.** (A) Genes identified in
1121 common between gut and brain at 9 and 35 months of age. B) Genes significantly altered at
1122 “early” and “late” stages of ageing in the gut (B1, 2) and brain (C1, 2), respectively. Network
1123 analysis was performed in STRING software and included the genes identified in the
1124 temporal profiles (from STEM) and in ALL DEGs. Red squares highlight the protein-protein
1125 interaction network of the gene changes that are accelerated in the *tert*^{-/-} (tert-dependent).

1126

1127

1128

1129

1130

1131

1132

1133

1134

1135

1136

1137

1138

1139

1140

1141

1142

1143

1144

1145

1146

1147

1148

1149

1150

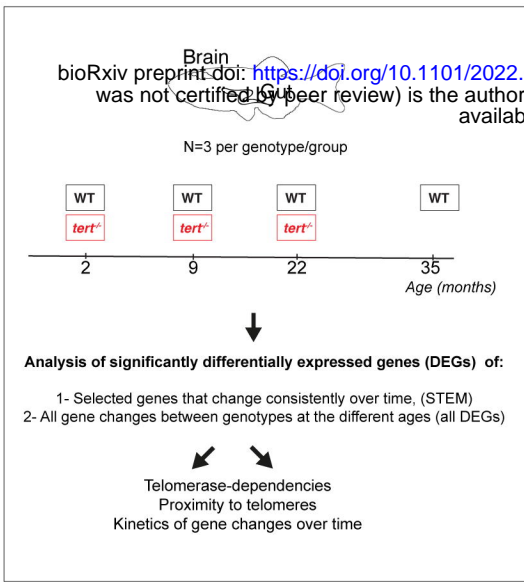
1151

1152

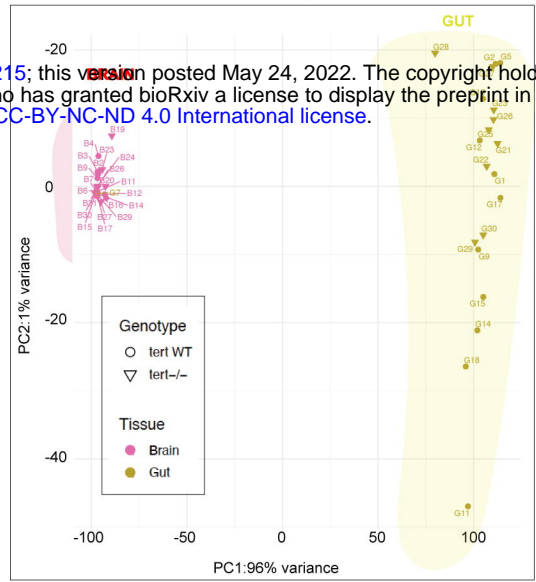
1153

1154

A) Study design



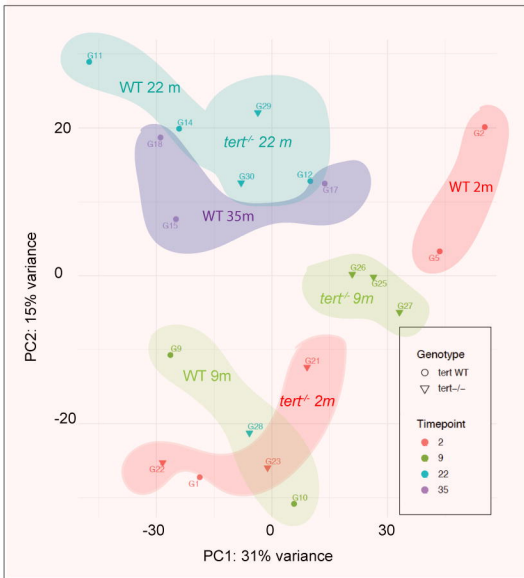
B) Principal Component Analysis (PCA) of all samples



C)



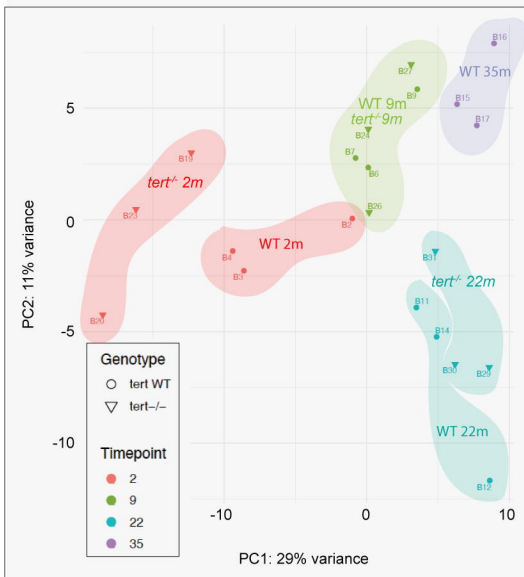
PCA of gut samples



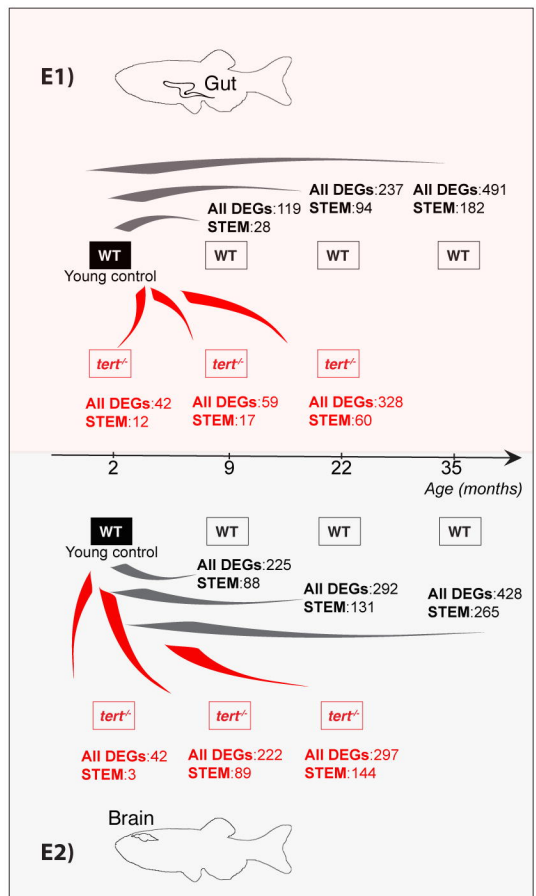
D)



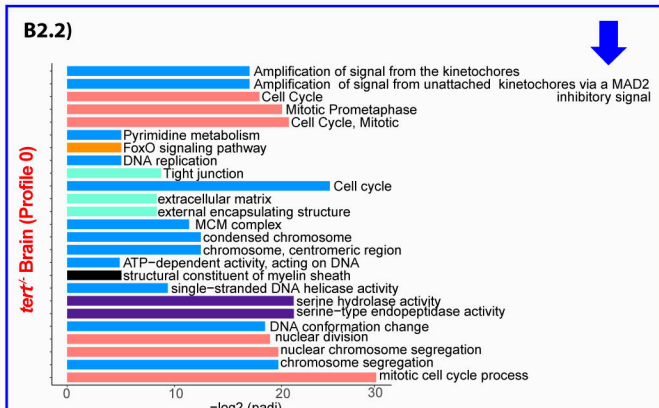
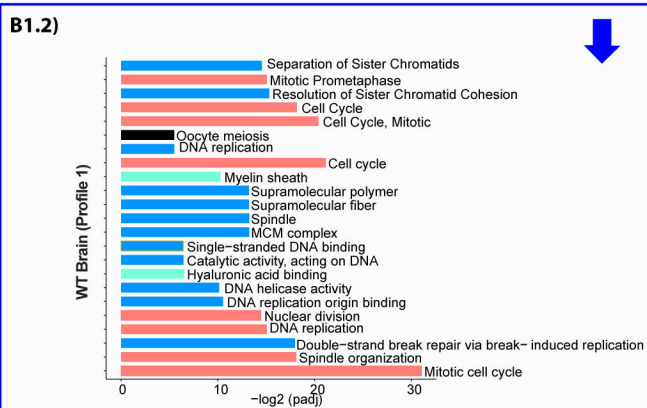
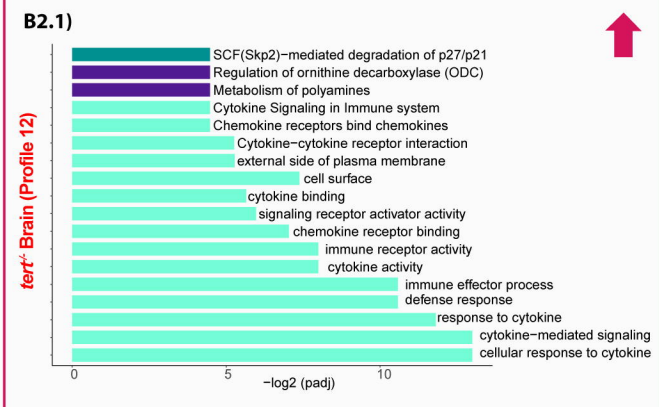
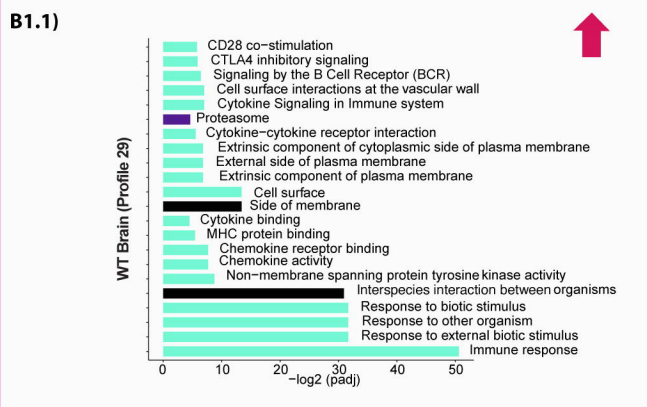
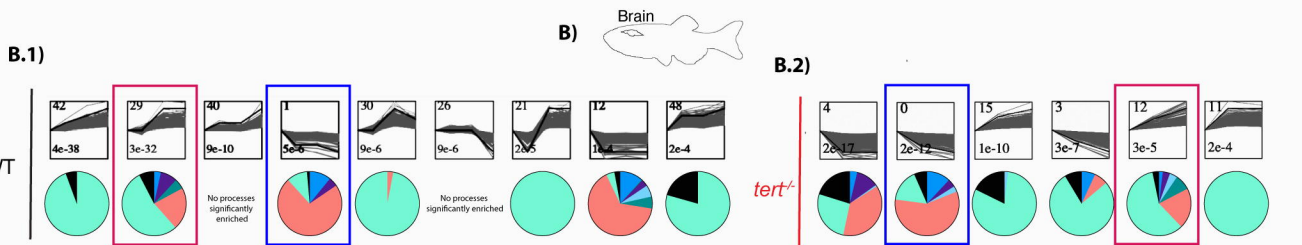
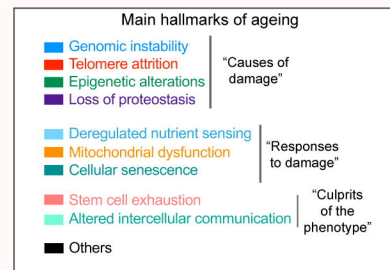
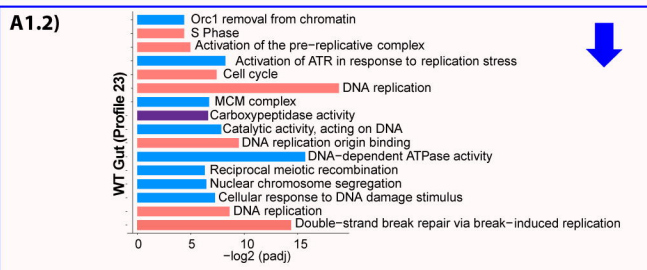
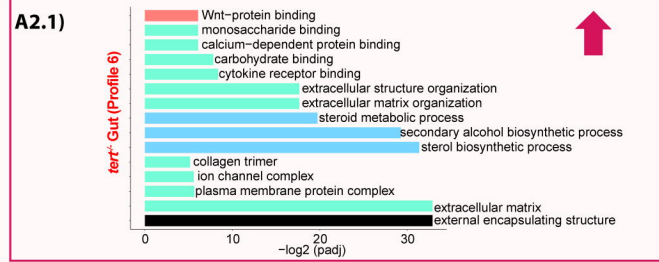
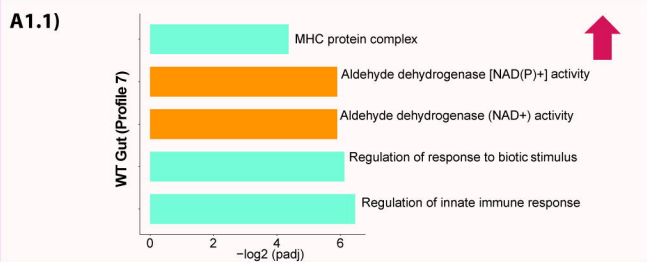
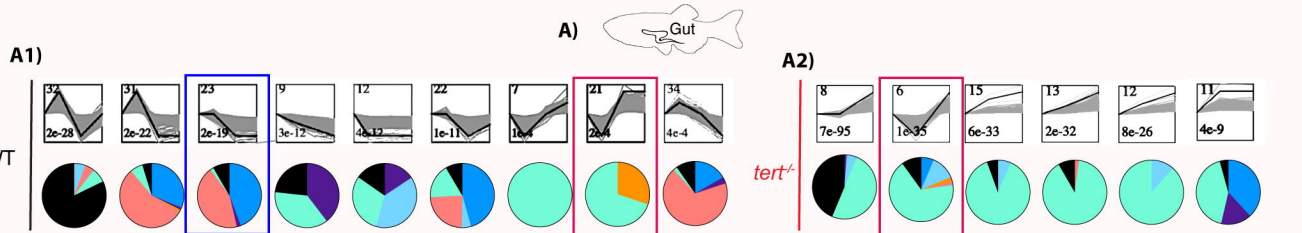
PCA of brain samples



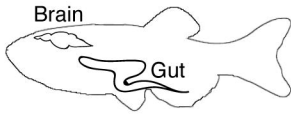
E) Summary of significant Differentially Expressed Genes (DEGs) numbers



Significant STEM profiles and main processes associated, categorised according to known hallmarks of ageing



Kinetics of ageing in the zebrafish gut and brain

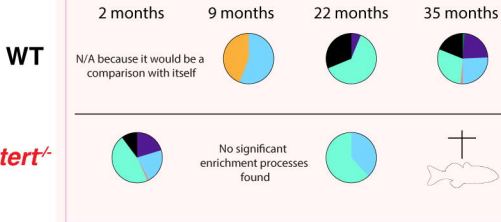


Main hallmarks of ageing affected

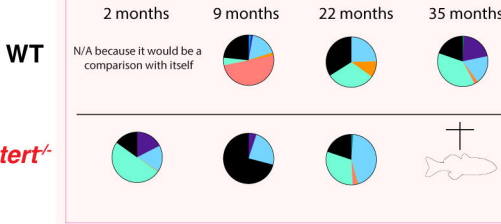
- Genomic instability
- Telomere attrition
- Epigenetic alterations
- Loss of proteostasis
- Deregulated nutrient sensing
- Mitochondrial dysfunction
- Cellular senescence
- Stem cell exhaustion
- Altered intercellular communication
- Others



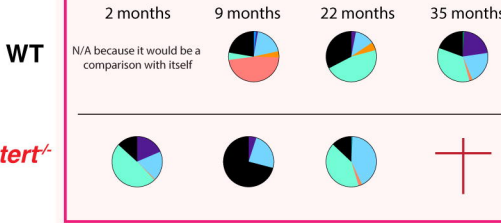
A1) From within the WT STEM profiles



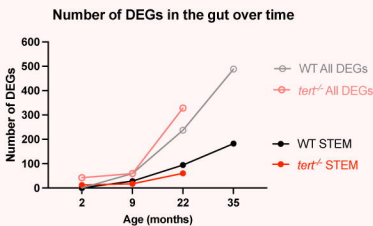
A2) From within ALL DEGs



A3) From within STEM & ALL DEGs combined



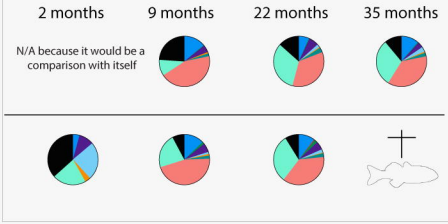
A4)



B1) From within the WT STEM profiles



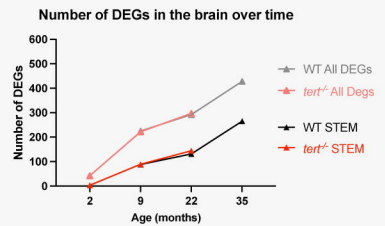
B2) From within ALL DEGs



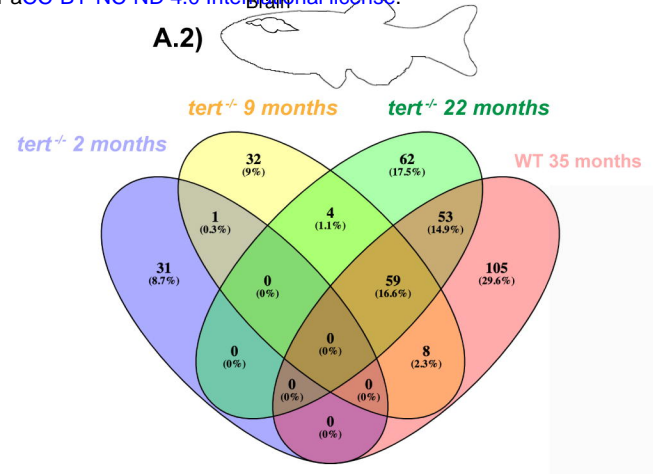
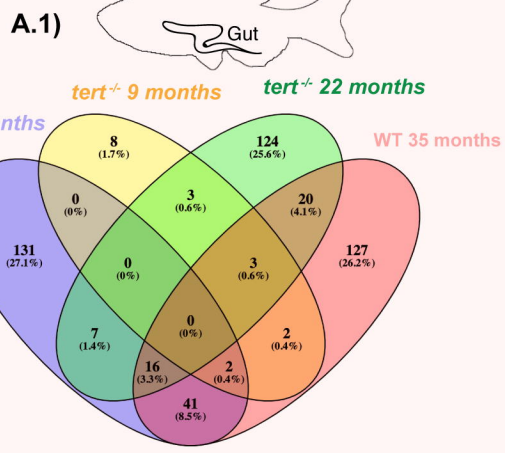
B3) From within STEM & ALL DEGs combined



B4)



A) Genes associated with the hallmarks of ageing in common between *tert*^{-/-} at the different ages and the aged WT at 35 months



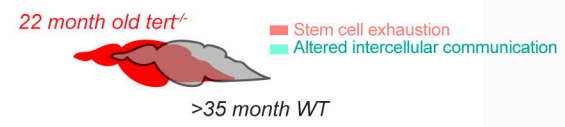
B) Most gene changes shared between *tert*^{-/-} and 35 month old WT, related to the main hallmarks of ageing affected

B.1) GUT



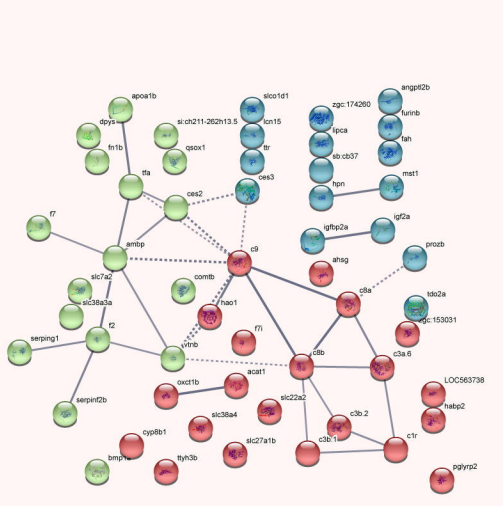
| | | |
|-------------------|----------------|--------------------------|
| <i>angptl2b</i> | <i>acat1</i> | <i>ahsg1</i> |
| <i>apoa1b</i> | <i>ces2a</i> | <i>ambp</i> |
| <i>c8a</i> | <i>ces3</i> | <i>bmp1a</i> |
| <i>c8b</i> | <i>comtb</i> | <i>c1r</i> |
| <i>c9</i> | <i>dpys</i> | <i>c3a.6</i> |
| <i>cyp8b1</i> | <i>fah</i> | <i>c3b.1</i> |
| <i>lcn15</i> | <i>hao1</i> | <i>c3b.2</i> |
| <i>pglyrp2</i> | <i>igtfa</i> | <i>f2</i> |
| <i>slc22a2</i> | <i>igtbp2a</i> | <i>f7</i> |
| <i>slc27a1b</i> | <i>lipca</i> | <i>f7i</i> |
| <i>slc38a3a</i> | <i>pla1a</i> | <i>fn1b</i> |
| <i>slc38a4</i> | | <i>furinb</i> |
| <i>slc7a2</i> | | <i>habp2</i> |
| <i>slco1d1</i> | | <i>hpn</i> |
| <i>tdo2a</i> | | <i>mst1</i> |
| <i>tfa</i> | | <i>oxct1b</i> |
| <i>ttr</i> | | <i>prozb</i> |
| <i>tyrh3b</i> | | <i>qsox1</i> |
| <i>vtnb</i> | | <i>sb.cb37</i> |
| <i>zgc:153031</i> | | <i>serpinf2b</i> |
| <i>zgc:174260</i> | | <i>serping1</i> |
| | | <i>si:ch211-262h13.5</i> |
| | | <i>si:ch211-284e20.8</i> |

B.2) BRAIN

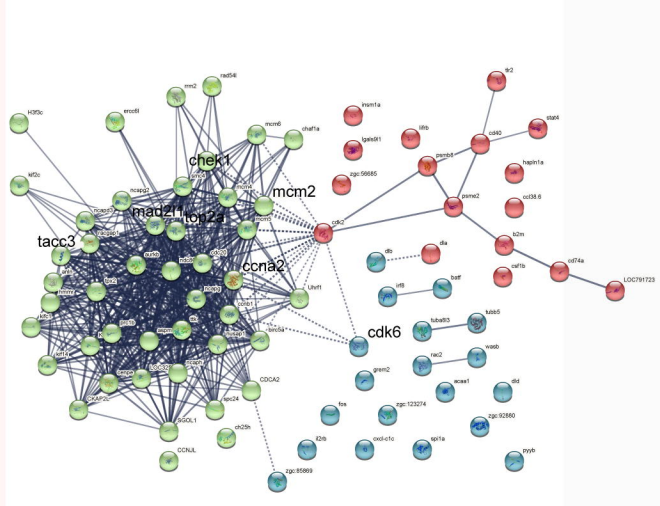


| | | | |
|-------------------|--------------------------|-----------------|--------------------------|
| <i>aspm</i> | <i>insm1a</i> | <i>kif11</i> | <i>acaa1</i> |
| <i>aurkb</i> | <i>mcm4</i> | <i>kif14</i> | <i>anln</i> |
| <i>birc5a</i> | <i>mcm5</i> | <i>kif20a</i> | <i>b2m</i> |
| <i>ccna2</i> | <i>mcm6</i> | <i>kif2c</i> | <i>balf</i> |
| <i>ccnb1</i> | <i>ncapg</i> | <i>kif4</i> | <i>cci38.6</i> |
| <i>ccnj1</i> | <i>ncapg2</i> | <i>kifc1</i> | <i>cd40</i> |
| <i>cdc20</i> | <i>ncaph</i> | <i>lgals9l1</i> | <i>cd74a</i> |
| <i>cdk2</i> | <i>nusap1</i> | <i>mad2l1</i> | <i>ch25h</i> |
| <i>cdk6</i> | <i>prc1b</i> | <i>mcm2</i> | <i>csf1b</i> |
| <i>cenpe</i> | <i>primpol</i> | <i>ncapd3</i> | <i>cxcl18b</i> |
| <i>chaf1a</i> | <i>rad54l</i> | <i>ndc80</i> | <i>grem2b</i> |
| <i>chek1</i> | <i>rm2</i> | <i>tuba8l3</i> | <i>h3f3b.1</i> |
| <i>ckap2l</i> | <i>sgo1</i> | | <i>h3f3c</i> |
| <i>dla</i> | <i>si:ch211-244o22.2</i> | | <i>hbba2</i> |
| <i>dlb</i> | <i>smc4</i> | | <i>il2rb</i> |
| <i>dld</i> | <i>spc24</i> | | <i>irf8</i> |
| <i>ercc6l</i> | <i>tacc3</i> | | <i>lifr</i> |
| <i>fosab</i> | <i>top2a</i> | | <i>lhfr</i> |
| <i>gadd45gb.1</i> | <i>tpx2</i> | | <i>mhc2a</i> |
| <i>h2af1al</i> | <i>ttk</i> | | <i>psmb8a</i> |
| <i>hapln1a</i> | <i>tubb5</i> | | <i>psme2</i> |
| <i>hmmr</i> | <i>uhf1</i> | | <i>pyyb</i> |
| | <i>wldhd1</i> | | <i>rac2</i> |
| | | | <i>racgap1</i> |
| | | | <i>si:busm1-266f07.2</i> |
| | | | <i>spi1a</i> |
| | | | <i>stat4</i> |
| | | | <i>tlr2</i> |
| | | | <i>wasb</i> |

B1.1) String Network analysis (K means clustering) GUT



B.2.1) String Network analysis (K means clustering) BRAIN



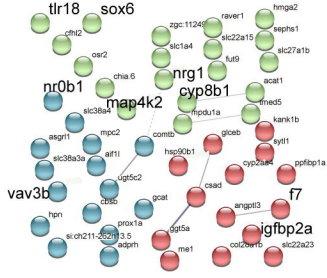
tert-dependent gene changes of old age



bioRxiv preprint doi: <https://doi.org/10.1101/2022.05.24.493215>; this version posted May 24, 2022. The copyright holder for this preprint (which was not certified by peer review) is the author/funder, who has granted bioRxiv a license to display the preprint in perpetuity. It is made available under aCC-BY-NC-ND 4.0 International license.

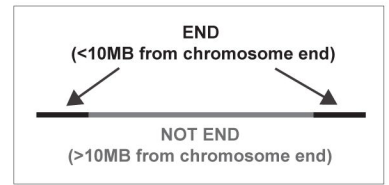


A1) Protein-protein interaction (PPI) network and cluster analysis

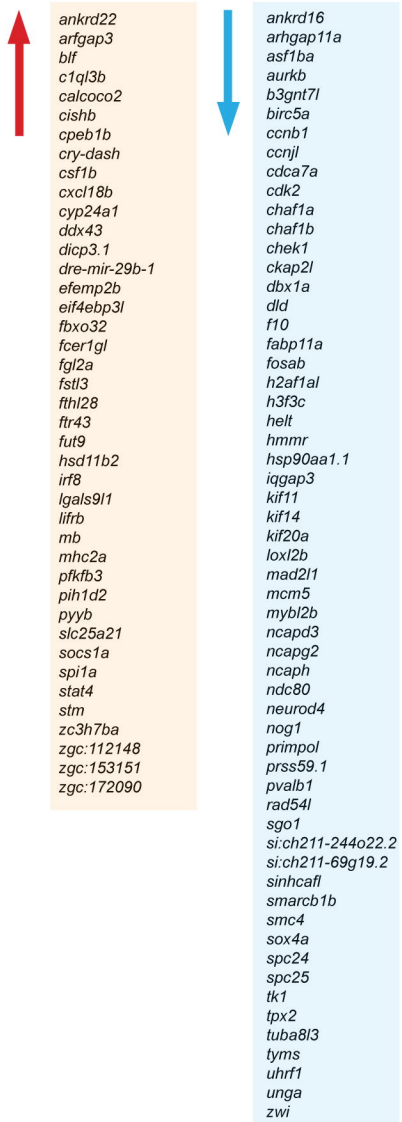
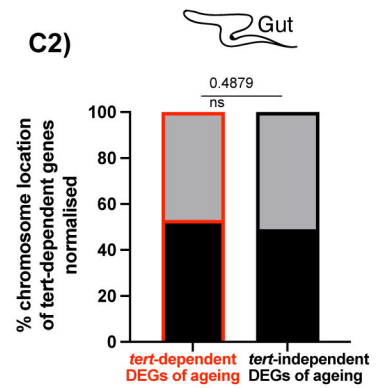


Organic acid metabolic process
Oxoacid metabolic process
Carboxylic acid metabolic process
Metabolic pathways
Monocarboxylic acid metabolic process
Taurine and hypotaurine metabolism
PPAR signaling pathway

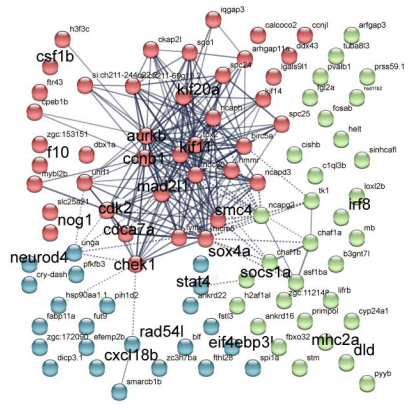
C1)



C2)

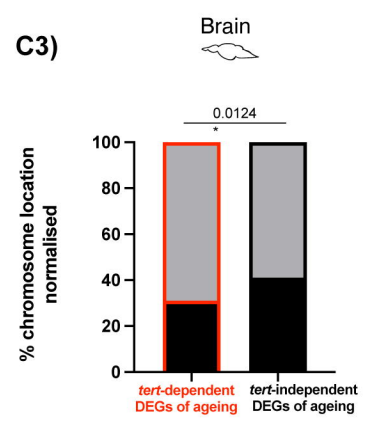


B1) Protein-protein interaction (PPI) network and cluster analysis

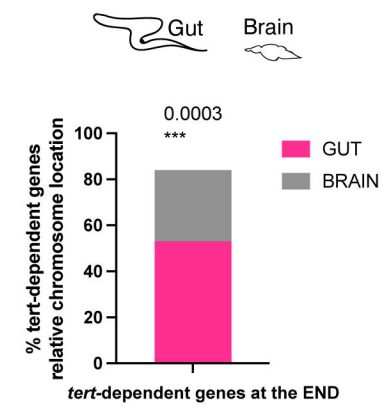


Cell cycle
genome stability
Immune system

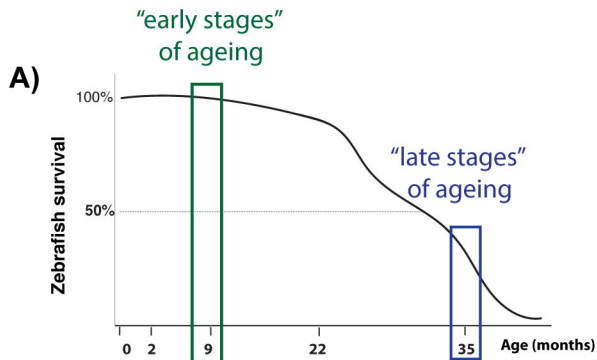
C3)



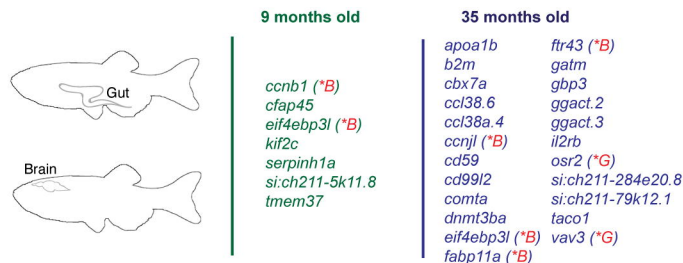
C4)



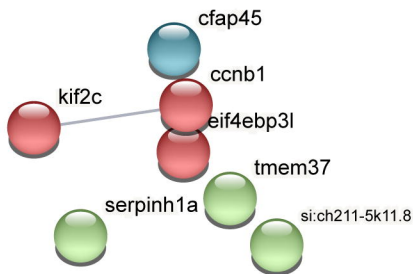
Protein-protein interaction (PPI) network and cluster analysis of changes in WT ageing (STEM and All DEGs combined)



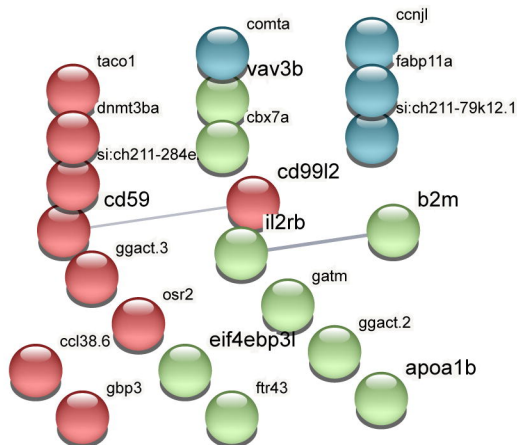
A.1) DEGs shared between gut and brain



B) PPI of DEGs shared between gut and brain at 9 months



C) PPI of DEGs shared between gut and brain at 35 months



A) Genes associated with the hallmarks of ageing in common between *tert*^{-/-} at the different ages and the aged WT at 35 months

A1)



WT 35 months x

***tert*^{-/-} 2 months**

acat1 sb:cb37
ahsg1 serpinf2b
ambp serping1
angptl2b si:ch211-262h13.5
apoa1b si:ch211-284e20.8
bmp1a slc22a2
c1r slc27a1b
c3a.6 slc38a3a
c3b.1 slc38a4
c3b.2 slc7a2
c8a slco1d1
c8b tdo2a
c9 tfa
ces2a ttr
ces3 ttyh3b
comtb vtnb
cyp8b1 zgc:153031
dpys zgc:174260
f2
f7
f7i
fah
fn1b
furinb
habp2
hao1
hbba1
hpn
igf2a
igfbp2a
lcn15
lipca
mst1
nr0b1
oxct1b
pglyrp2
pla1a
prox1a
prozb
qsxo1

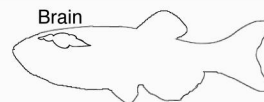
***tert*^{-/-} 9 months**

acsf2
cyp8b1
hbba2
mgll
p4ha2
pla1a
sephs1

***tert*^{-/-} 22 months**

acat1
anppl3
comtb
f10
f7
fam83d
gatm
gbp3
gcat
ggf5a
glyctk
gpt
hpn
itln2
me1
misl
mpc1
nr0b1
nrg1
oaz2a
pcbd1
pcxa
pkf1b
prox1a
si:ch211-262h13.5
si:ch211-284e20.8
slc16a6a
slc1a4
slc27a1b
slc38a3a
slc38a4
slc43a1b
slc7a2
slco1d1
ttr
tyh3b
urahb
vkorc1
zgc:92040

A2)



WT 35 months x

***tert*^{-/-} 9 months**

anln
arhgap11a
aspm
aurkb
ccna2
ccnb1
cd40
cdc20
cdk2
cdk6
cenpe
chaf1b
cyp24a1
dbx1a
dld
dnmt3aa
dnmt3ba
ercc6l
f10
gadd45gb.1
hapln1a
hsp90aa1.1
igf2bp1
insm1a
kif11
kif14
kif20a
kif2c
kif4
kifc1
lifr
mad2l1
marcksa
mbpb
mcm2
mcm5

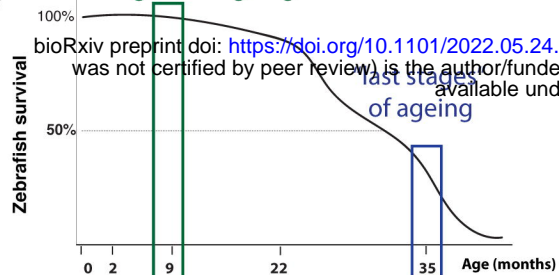
mcm6
mybl2b
ncapd3
ncapg
ncapg2
ncaph
ndc80
neurod4
nusap1
orc3
plp1b
primpol
rrm2
sgo1
si:ch211-244o22.2
smc4
socs1a
sox4a
sox4b
spc24
spc25
spi1a
tacc3
top2a
tpx2
ttk
tubb5
tyms
uhrf1
unga

***tert*^{-/-} 22 months**

acaa1
anln
asf1ba
aspm
aurkb
b2m
balf
birc5a
ccl38.6
ccna2
ccnb1
ccnj1
cd40
cd74a
cdc20
cdk2
cdk6
cenpe
ch25h
chaf1a
chaf1b
chek1
ckap2l
csf1b
cxcl18b
dbx1a
dla
dlb
dld
dnmt3aa
dnmt3ba
ercc6l
fosab
foxn4
gadd45gb.1
grem2b
h2af1al
h3f3b.1
h3f3c
hapln1a
hbba2
hbba2
hmmr
igf2bp1
il2rb
inab
insm1a
irf8
kif11
kif14
kif20a
kif2c
kif4
kifc1
lgals9l1
lifr
mad2l1
marcksa
mbpb
mcm2
mcm4
mcm5
mcm6
mhc2a
mybl2b
ncapd3
ncapg
ncapg2
ncaph
ndc80
nefmb
neurod4
nusap1
plp1a
plp1b
ppp1r14ba
prc1b
prdm8
primpol
psmb8a
psme2
pyyb
rac2
racgap1
rad54l
rrm2
sgo1
si:busm1-266f07.2
si:ch211-244o22.2
smarcb1b
smc4
sox11a
sox4a
sox4b
spc24
spi1a
spinb
stat4
tacc3
tap2a
tlr2
top2a
tpx2
ttk
tuba8l3
tubb5
tyms
ube2c
uhrf1
wasb
wdhd1
zwi

Protein-protein interaction network and cluster analysis of changes in WT ageing (STEM and All DEGs combined)

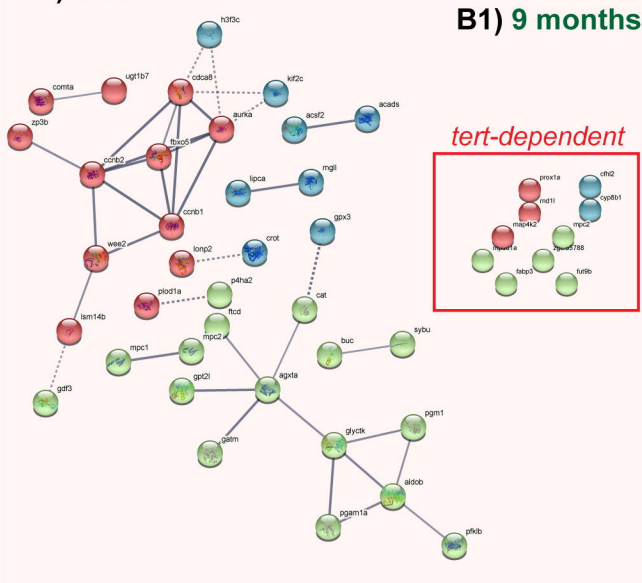
A) "origins" of ageing



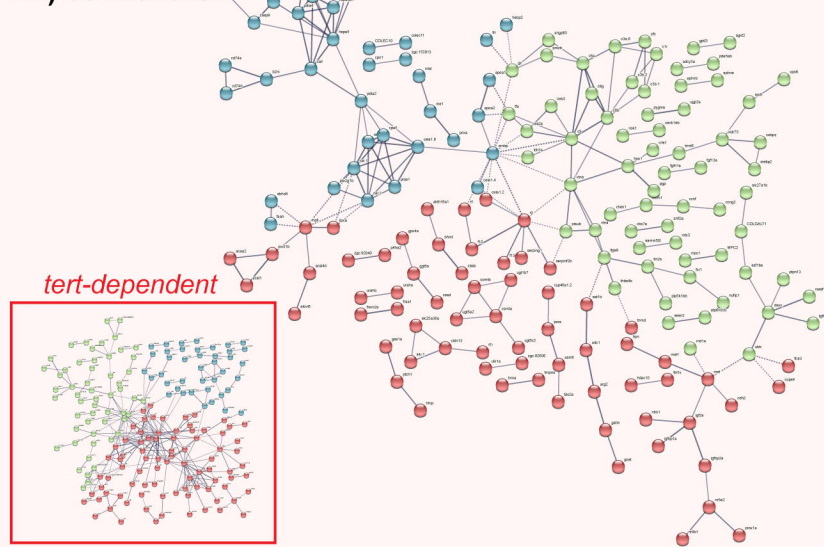
A.1) DEGs shared between gut and brain



B) GUT

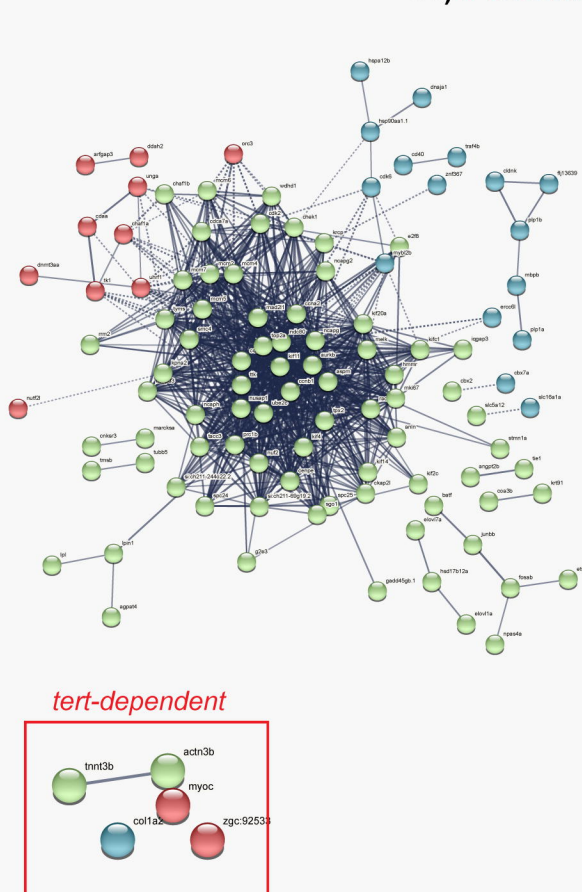


B2) 35 months



C) BRAIN

C1) 9 months



C2) 35 months

